Biogeosciences Discuss., 5, 4621–4680, 2008
www.biogeosciences-discuss.net/5/4621/2008/

Biogeosciences Discussions

Biogeosciences Discussions is the access reviewed discussion forum of *Biogeosciences*

Use of laboratory and remote sensing techniques to estimate vegetation patch scale emissions of nitric oxide from an arid Kalahari savanna

G. T. Feig[1], B. Mamtimin[2], and F. X. Meixner[3]

[1]Max Planck Institute for Chemistry, Biogeochemistry Department P.O. Box 3060, 55020 Mainz, Germany
[2]Department of Physics University of Zimbabwe, Harare, Zimbabwe
[3]Institute of Geography Science and Tourism, Xinjiang Normal University, P.R. China

Received: 15 September 2008 – Accepted: 6 October 2008 – Published: 3 December 2008

Correspondence to: G. Feig (feig@mpch-mainz.mpg.de)

Published by Copernicus Publications on behalf of the European Geosciences Union.

Abstract

The biogenic emission of nitric oxide (NO) from the soil has an important impact on a number of environmental issues, such as the production of tropospheric ozone, the cycle of the hydroxyl radical (OH) and the production of NO. In this study we collected soils from four differing vegetation patch types (Pan, Annual Grassland, Perennial Grassland and Bush Encroached) in an arid savanna ecosystem in the Kalahari (Botswana). A laboratory incubation technique was used to determine the net potential NO flux from the soils as a function of the soil moisture and the soil temperature. The net potential NO emissions were up-scaled for the year 2006 and a region (185 km × 185 km) of the southern Kalahari. For that we used (a) the net potential NO emissions measured in the laboratory, (b) the vegetation patch distribution obtained from Landsat NDVI measurements, (c) estimated soil moisture contents obtained from ENVISAT ASAR measurements and (d) the soil surface temperature estimated using MODIS MOD11A2 8 day land surface temperature measurements. Differences in the net potential NO fluxes between vegetation patches occur and range from 0.27 ng m^{-2} s^{-1} in the Pan patches to 2.95 ng m^{-2} s^{-1} in the Perennial Grassland patches. Up-scaling the net potential NO fluxes with the satellite derived soil moisture and temperature data gave NO fluxes of up to 323 g ha^{-1} $month^{-1}$, where the highest up-scaled NO fluxes occurred in the Perennial Grassland patches, and the lowest in the Pan patches. A marked seasonal pattern was observed where the highest fluxes occurred in the austral summer months (January and February) while the minimum fluxes occurred in the austral winter months (June and July), and were less than 1.8 g ha^{-1} $month^{-1}$. Over the course of the year the mean NO emission for the up-scaled region was 0.54 kg ha^{-1} yr^{-1}, which accounts for a loss of up to 7.4% of the nitrogen (N) input to the region through atmospheric deposition and biological N fixation. The biogenic emission of NO from the soil is therefore an important mechanism of N loss from this arid savanna ecosystem and has the potential to play an important role in the production of tropospheric ozone and the OH cycle.

BGD

5, 4621–4680, 2008

1 Introduction

The concentrations of nitric oxide (NO) and nitrogen dioxide (NO_2) (collectively known as NO_x) are important in regulating chemical reactions of the atmosphere (Crutzen, 1995; Crutzen and Lelieveld, 2001; Monks, 2005). They control the production and destruction of tropospheric ozone (Chameides et al., 1992; Crutzen and Lelieveld, 2001), are involved in the cycle of the OH radical (the most important tropospheric cleansing agent) and in the production of nitric acid (HNO_3) (Logan, 1983; Meixner, 1994; Monks, 2005; Steinkamp et al., 2008). The global emissions of NO_x have been severely altered by anthropogenic activity. In 1860 global NO_x emissions were estimated to be 13 Tg yr^{-1} of which the majority is thought to have come from natural sources such as soils and lightning (Galloway et al., 2004). The recent estimate of the IPCC puts total NO_x emissions at 42–47 Tg yr^{-1} with the most important source being fossil fuel combustion (Denman et al., 2007), and soil is thought to account for between 10% to 40% of the total NO emissions (Davidson and Kingerlee, 1997; Denman et al., 2007). Over 40% of the total NO emissions from Africa are supposed to originate from biogenic production in the soil (Jaegle et al., 2004). The wide range of uncertainty is partly due to insufficient measurements, particularly in the drylands (Galbally et al., 2008). A recent review by Meixner and Yang (2006) only identified 13 studies in natural ecosystems receiving less than 400 mm rain a year (since then three other studies have occurred (Feig et al., 2008; Holst et al., 2007; McCalley and Sparks, 2008), this is problematic since drylands make up a sizable proportion of the earth's surface area and are thought to be capable of substantial emissions of NO (Davidson and Kingerlee, 1997).

The biogenic production of NO in the drylands is dominated by the process of nitrification (Conrad, 1996; Galbally et al., 2008). Nitrification is influenced by environmental factors, such as the soil moisture, the soil temperature and the soil nutrient content. These in turn are determined through the underlying geology, the climate and biotic factors such as the vegetation at the site (Brümmer et al., 2008; Davidson, 1991b; Galbally et al., 2008; Garrido et al., 2002; Ludwig et al., 2001; Russow et al., 2000).

BGD
5, 4621–4680, 2008

In drier ecosystems, soil water seems to be the most important factor regulating emissions of NO. When the soil moisture is too low to maintain microbial activity there are very low levels of NO emitted (Galbally et al., 2008; Garrido et al., 2002; Meixner et al., 1997) and when soil moisture levels are too high to maintain aerobic conditions, the emission of NO is negligible (Skopp et al., 1990). The optimal emission of NO in drylands seems to occur at low soil moisture levels, but where microbial activity can still take place. In a previous laboratory based study in the Kalahari, NO emissions were very low at both high and low soil moisture contents, while the optimum soil moisture for NO production was approximately 20% Water Filled Pore Space (WFPS) (Aranibar et al., 2004). Since the biogenic production of NO is mostly a bacterially mediated process, temperature has an important impact on the rate of the reaction, and as the environmental temperature increases so does the rate of nitrification and hence the release of NO. A number of previous studies have shown that the rate of NO increase approximately doubles with a 10°C increase in temperature (Feig et al., 2008; Kirkman et al., 2001; McCalley and Sparks, 2008). The soil nutrient status is another important controller of biogenic NO emissions; many studies have found a relationship between the emissions of NO and either the concentrations of ammonia or nitrate (Erickson et al., 2002, 2001; Hartley and Schlesinger, 2000; Hutchinson et al., 1993; Ludwig et al., 2001; Meixner et al., 1997; Parsons et al., 1996) or the N cycling rate (Erickson et al., 2002, 2001; Hartley and Schlesinger, 2000; Parsons et al., 1996). Therefore, natural or anthropogenic actions that result in the modification of the inputs of nutrients or the rates of nutrient turnover are likely to have an effect on the NO production rates.

The Kalahari ecosystem extends from South Africa, through Botswana and into Zambia and covers an area of 2.5 million km^2, it is an ecosystem occurring on a homogenous substrate. A rainfall gradient exists, from approximately 200 mm yr^{-1} in the south to over 1000 mm yr^{-1} in the north, this results in a gradient of vegetation, from sparse arid fine leaved bush-savanna representing nutrient rich ecosystems in the south; to nutrient poor broad leaved Miombo woodland in the north (Aranibar et al., 2004; Scholes and Parsons, 1997).

BGD
5, 4621–4680, 2008

The Kalahari is currently undergoing extensive land use change associated with an increase in pastoral land use, which has been made possible with the introduction of boreholes to provide water for livestock. Grazing is concentrated around the permanent water sources and creates a distinctive disturbance pattern of concentric vegetation zones. Typically in the close vicinity to the water source there is what has been termed the "sacrifice zone" where there is heavy disturbance; this is followed by a "bush encroached" where there is a strong increase in the proportion of woody shrub vegetation, typically dominated by (*Acacia mellifera*) (Dougill and Thomas, 2004; Hagos and Smit, 2005; Thomas and Dougill, 2007) resulting from the preferential use of grass species by cattle. Beyond the bush encroached zone, where there is less disturbance, the later successional stages of vegetation occur.

The vegetation is known to have an effect on the quantity and cycling of nutrients (Hagos and Smit, 2005). This has been shown to influence the emission of NO from the soil, for example in Texas the emission of NO is higher under areas where there has been encroachment of *Prosopis* sp. (Hartley and Schlesinger, 2000; Martin and Asner, 2005; Martin et al., 2003a). These previous studies have either looked at the larger landscape scale (Aranibar et al., 2004; Brümmer et al., 2008; Davidson, 1991a; Delon et al., 2007; Hartley and Schlesinger, 2000; Jaegle et al., 2004; Martin et al., 2003b; Otter et al., 1999; Serca et al., 1998) or at the vegetation canopy scale (Barger et al., 2005; Hall and Asner, 2007; Hartley and Schlesinger, 2000; Holst et al., 2007; Le Roux and Abbadie, 1995; Levine et al., 1996; Martin et al., 1998; McCalley and Sparks, 2008; Meixner et al., 1997; Mosier et al., 2003; Smart et al., 1999); however there is a need to determine what occurs in the emission of NO between the plant canopy scale and the vegetation patch scale which has been examined in only very few studies (Kirkman et al., 2001; Martin and Asner, 2005; Scholes et al., 1997; Van Dijk et al., 2002). The main points of consideration in this study are (1) to determine the effect of differing vegetation cover types on the emission of NO along a disturbance gradient and (2) attempt to up-scale point measurements of NO release to a regional emission estimate for NO flux from the soil.

2 Methods and materials

2.1 Site

The site of the research was at the Berry Bush Farm (25°56′47.73 S, 22°25′39.47 E, elevation 978 m), a 900 ha commercial ranch, situated approximately 10 km north east of the town of Tsabong in the Kgalagadi District, Botswana. The ranch was formerly used for cattle and sheep farming but at the time of sampling, in May 2006, the stock densities had been reduced and it was only grazed by approximately 120 springbok and other small game. The area has been described as a grass bush savanna (Dougill and Thomas, 2004) and is situated on the southern portion of the Kalahari sands. The soils in the Kalahari sands are typically deficient in nutrients, deep, structureless and consist of an average of 62% fine quartz sand in all horizons (Ringrose et al., 1998).

The Kalahari is in a highly seasonal (austral) summer rainfall region, with very high inter-annual variability (Thomas and Dougill, 2007). Mean rainfall measured at the official meteorological station at Berry Bush Farm is 280 mm yr^{-1} with a 32% annual variability for the period 1997–2005 (Keith Thomas, personal communication). At the Tsabong WMO station (WMO Index number 68328) it has been reported that it has a mean annual rainfall of approximately 300 mm with a 45% inter-annual variability (Thomas and Dougill, 2007). The year of sampling, 2006, was a very wet year and 418 mm of rain had fallen by the time the soil samples were taken in May.

Four main types of vegetation patches occur on the Berry Bush Farm and are thought to represent a repeated vegetation pattern for the region. The four vegetation patches are; Annual Grassland, Perennial Grassland, bush Encroachment and Pan. From the four main types of vegetation patches that occur on the Berry Bush Farm three of the patches, namely; Perennial Grassland, Annual Grassland and Encroachment correspond to differing successional stages in the disturbance regime (where the Perennial Grassland is the least disturbed and the Encroachment is the most disturbed).

BGD
5, 4621–4680, 2008

2.2 Soil and vegetation sampling

Three replicate sampling sites were selected in each of the vegetation patch types. At each of the sampling sites three 25 m transects were laid out at 120° to each other. The plant cover was estimated as the vegetation cover directly over the transect line and was assigned to various vegetation structural classes, if more than one structural unit overlapped, the larger more physically dominant was recorded. Six different vegetation structural classes have been defined which consisted of; perennial grasses, annual grasses (grasses were classified as annual or perennial species according to Van Oudtshorn (1999)), tree cover, soil crusts, bare soil and other (including shrubs and forbs). For each of the vegetation patch types the total aerial cover was estimated from the sum of the nine transects (three replicates of each vegetation patch and three 25 m transects within each replicate).

In each of the sampling sites ten soil samples (approx. 150 g) were taken under each of three vegetation types; tree cover, grass cover and open, these were then combined to make a representative soil sample of approximately 1.5 kg in mass (four vegetation patches, three replicates of each vegetation patch, and three vegetation types giving a total of thirty nine 1.5 kg soil samples). In the Pan ten soil sub-samples were also taken under soil crust. The soil crusts were defined according to the classification of Dougill and Thomas (2004), however only the second and third stage crusts were sampled, since these were the most developed and were clearly discernable. The soil was air dried, sieved through 2 mm mesh and stored at 5°C until use. Within each of the vegetation types the soil bulk density was measured in the first 5 cm using a stainless steel soil core of known volume.

The soil texture was determined using a hydrometer technique after the method of (Day, 1969) and the soil pH was measured in 2.5:1 mixture in distilled water according to the method of Anderson; and Ingram (1993). Soil samples were sent to the micro analytical laboratory at the University of Mainz where total soil carbon (C) and soil nitrogen (N) content was measured using a Vario MICRO Cube universal microanalyser

BGD
5, 4621–4680, 2008

set up to measure total C, and N contents of the soil.

2.3 Laboratory incubation and net NO release from soil

Two days before beginning the measurements, the soil was soaked with deionised water and allowed to drain freely at room temperature (22°C), this was to limit the confounding effect of pulsing after the initial wetting of soil after a long period of inactivity. Pulsing is known to elicit a large but temporally limited emission. The magnitude of the pulse after rewetting the soil is variable depending on the preceding period of time in which the soil was dry. Since this can not be easily controlled and pulsing is thought to add a fairly minor contribution to the annual NO flux, reported to be less than 6% (Scholes et al., 1997) we decided to neglect the effect of pulsing in this study, which means that the fluxes that are calculated here should be considered to be a lower limit. The basic methodology for the laboratory measurement of the NO flux from soil has been previously described (Aranibar et al., 2004; Kirkman et al., 2001; Meixner and Yang, 2006; Otter et al., 1999; Van Dijk et al., 2002) and was further developed by Feig et al. (2008). It has been shown that there is good agreement between laboratory fluxes of NO calculated according to this method and the measured field fluxes (Ludwig et al., 2001; Meixner et al., 1997; Van Dijk et al., 2002). Briefly; a known quantity (approximately 100 g (dry weight)) of sieved, wetted soil was placed in one of five plexiglas chambers (volume 0.97 l) in a thermo-controlled cabinet. Pressurised air that had passed through a purification system was supplied to each chamber at a flow rate of 4.2×10^{-5} m^3 s^{-1} (2.5 L min^{-1}). The outlet of each chamber was connected via a reversed Naphion drier (series MD-110, Perma Pure LLC, USA) and a switching valve to a NO Chemoluminescence analyser (CLD780TR, Eco Physics Switzerland) and a H_2O/CO_2 analyser (Binos IR gas analyser, Rosemont Analytical, USA). Nitric oxide standard gas (200 ppm) was attached to the air purification system via a mass flow controller and diluted into the "zero"-gas stream; this allowed (1) the calibration of the chemoluminescence analyser and (2) for the control of the headspace NO mixing ratio when determining NO uptake in the soil (see below). The soil moisture content

was determined by integrating the loss of water vapour throughout the measurement period and relating it to the gravimetric soil moisture content at the start and end of the measurement.

2.4 Measurements of the net NO release rate

The net release of NO (J_{NO}, in ng kg^{-1} s^{-1}) (all units are in terms of mass of N and dry mass of soil) is calculated from the difference between the NO mixing ratio at the outlet of the reference cuvette and the outlet of each of the incubation cuvettes (since the air in the cuvette is well mixed by a microfan, the air at the outlet is assumed to have the same composition as the air in the headspace) according to:

$$J_{NO} = \frac{Q}{M_{soil}} \left(m_{NO,out} - m_{NO,ref}\right) \times \left(\frac{M_N}{V_m} \times 10^{-3}\right) \quad (1)$$

Where Q is the flow rate through the cuvette (4.2×10^{-5} m^3 s^{-1} or 2.5 L min^{-1}), M_{soil} is the dry mass of the soil (kg), M_N is the molar mass of N (14.0076 kg kmol^{-1}), V_m is the molar volume (24.465 m^3 kmol^{-1} at 25°C, 1013.25 hPa) and $m_{NO,ref}$ and $m_{NO,out}$ are the mixing ratios of NO in ppb, at the outlets of the reference and incubation cuvettes, respectively. The factor $M_N/V_m\times10^{-3}$ is needed to convert NO mixing ratio (ppb) to NO concentration (ng m^{-3}).

The release of NO from the soil is the result of the microbial production and consumption of NO in the soil, processes that occur simultaneously (Conrad, 1994, 1996; Conrad and Smith, 1995). As a result, the NO release rate (J_{NO}) is always a net release rate. However if the NO consumption is greater than production in the soil sample then J_{NO} becomes negative. This will only occur if the in-coming (= reference) NO mixing ratio is greater than the headspace NO mixing ratio in the soil containing chamber.

It has already been shown experimentally that there is a linear relationship between the NO release rate (J_{NO}) and the rates of NO production (P) and NO consumption (k) (Ludwig et al., 2001; Remde et al., 1989) so that the measured release rates can be

BGD
5, 4621–4680, 2008

described according to:

$$J_{NO} = P - k \times m_{NO,out} \times \left(\frac{M_N}{V_m} \times 10^{-3} \right) \quad (2)$$

This equation implies that the NO production is independent of the NO mixing ratio in the headspace ($m_{NO,out}$), while the NO consumption is dependent on the NO mixing ratio in the headspace, and can be approached as a first order decay process. To determine the values of P and k, Eq. (2) was used with the measured release rates (J_{NO}) from two sets of incubation measurements, namely using $m_{NO,ref,low}$=0 ppb and $m_{NO,ref,high}$=58 ppb. This allowed us to calculate P (ng kg^{-1} s^{-1}) and k (m^3 kg^{-2} s^{-2}), where k can be determined from the slope of Eq. (2),

$$k = \frac{\Delta J_{NO}}{\Delta [NO]} = \frac{J_{NO,high} - J_{NO,low}}{m_{NO,high} - m_{NO,low}} \times \left(\frac{V_m}{M_N} \times 10^3 \right) \quad (3)$$

Where $m_{NO,low}$ is the actual NO mixing ratio (ppb) in the head space of the cuvette under fumigation with NO free air and $m_{NO,high}$ is the actual NO mixing ratio in the cuvette headspace under fumigation with 58 ppb NO. In this study, we will present values of the NO release rate (J_{NO}) as a function of soil moisture, in terms of the soil WFPS. Water filled pore space is a useful concept because it indicates the amount of water in the soil that is available for microbial activity and also the amount of air in the soil (and therefore the soil oxygen status). The WFPS is calculated (a) from the amount of water lost from the enclosed cuvettes through evaporation during the incubation process and (b) through determining the gravimetric water content (Θ) of the wetted sample at the start of the incubation. The WFPS is calculated according to Eq. (4):

$$\text{WFPS} = \Theta \times \frac{BD}{\left(1 - \frac{BD}{PD}\right)} \quad (4)$$

Where BD is the soil bulk density in (kg m^{-3}) measured at the site of sampling, by driving a stainless steel core of known volume into the soil and removing a soil sample

BGD
5, 4621–4680, 2008

and drying the soil at 105°C for 48 h, and *PD* is the particle density of the average soil mineral (quartz) with a value of 2.65×10^3 kg m^{-3} according to (Parton et al., 2001).

2.5 Calculation of the net potential NO flux

The laboratory derived net release of NO (J_{NO}, in ng kg^{-1} s^{-1}) from the soil was converted to a net potential NO flux (F_{lab}, in ng m^{-2} s^{-1}) using a simple diffusion based algorithm (Eq. 5), originally developed by (Galbally and Johansson, 1989), modified by van Dijk et al. (2002). The net potential laboratory NO flux, as a function of WFPS and T_{soil}, is calculated according to:

$$F_{lab}(T_{soil}, \mathrm{WFPS}) = \sqrt{BD \times k(T_{soil}, \mathrm{WFPS}) \times D(\mathrm{WFPS})} \times \left(\frac{P(T_{soil}, \mathrm{WFPS})}{k(T_{soil}, \mathrm{WFPS})} \right) - [\mathrm{NO}]_{\mathrm{Headspace}} \quad (5)$$

Where $[\mathrm{NO}]_{\mathrm{Headspace}}$ is the NO concentration (in 10^{-12} kg m^{-3}) in the headspace of the cuvette; D(WFPS), in m^2 s^{-1}, is the WFPS dependent diffusion coefficient of NO through the soil, calculated after Moldrup et al. (2000), from the WFPS and the gas diffusion constant for free air (m^2 s^{-1}) equal to 1.9×10^{-5} m^{-2} s^{-1} (Gut et al., 1998). The diffusion coefficient is dependent of the soil moisture content and the soil bulk density and therefore is calculated for each soil sample and each soil moisture interval.

For a given soil temperature, an algorithm has been developed (Meixner and Yang, 2006) to fit our net potential NO fluxes as a function of the WFPS (Eq. 5). This algorithm describes the net potential NO flux as a power increase until optimal soil moisture followed by an exponential decrease:

$$F_{lab}(T_{soil} = \mathrm{const.}, \mathrm{WFPS}) = a\mathrm{WFPS}^b \exp(-c\mathrm{WFPS}) \quad (6)$$

Where parameters a, b and c are related to observed values by:

$$a = \frac{F_{lab}(\mathrm{WFPS}_{opt})}{\left[\mathrm{WFPS}_{opt}^b \exp(-b)\right]} \quad (7)$$

BGD
5, 4621–4680, 2008

$$b = \frac{\ln\left[\frac{F_{lab}(WFPS_{opt})}{F_{lab}(WFPS_{upp})}\right]}{\ln\left(\frac{WFPS_{opt}}{WFPS_{upp}}\right) + \frac{WFPS_{upp}}{WFPS_{opt}} - 1} \quad (8)$$

$$c = \frac{-b}{WFPS_{opt}} \quad (9)$$

Where, for a given T_{soil}, $WFPS_{opt}$ is the soil moisture where the maximum laboratory NO release is observed, $F_{lab}(WFPS_{opt})$ is the maximum net potential NO flux at the $WFPS_{opt}$ (the optimum WFPS), and $WFPS_{upp}$ is the soil moisture content where F_{lab} approximately equals zero (i.e. F_{lab} $(WFPS_{upp})=1/100\,F_{lab}$ $(WFPS_{opt})$ for $WFPS>WFPS_{opt}$).

The temperature dependence of the laboratory NO flux was determined by calculating the net potential NO flux at two soil temperatures, 25°C and at 35°C. The temperature dependence usually shows an exponential increase and can be expressed as the increase of F_{lab} for a 10°C increase in soil temperature, otherwise known as a Q_{10} function (Eq. 10) (Lloyd and Taylor, 1994).

$$Q_{10}(WFPS)=\frac{F_{lab}(T_{soil}=35°C, WFPS)}{F_{lab}(T_{soil}=25°C, WFPS)} \quad (10)$$

The Q_{10} function can then be included into Eq. (6), as a "temperature amplification factor" of the reference NO flux (T_{ref}=25°C), so that the laboratory NO flux can be estimated as a function of both soil temperature and soil moisture (Eq. 11):

$$F_{lab}(T_{soil}, WFPS)=a_{T_{ref}} WFPS^{b_{T_{ref}}} \exp\left(-c_{T_{ref}} \times WFPS\right) \times \exp\left[\frac{\ln Q_{10}(WFPS)}{10} \times (T_{soil}-T_{ref})\right] \quad (11)$$

2.6 Compensation point mixing ratio

The compensation point mixing ratio ($m_{NO,comp}$) is an important concept for the bidirectional exchange of NO (see (Conrad, 1994)). Since it determines what the ambient

mixing ratio of NO in the atmosphere has to be before a net NO uptake into the soil can occur. The compensation point mixing ratio is calculated by resolving Eq. (5) for the NO concentration where $F_{lab}(WFPS,T_{soil})=0$:

$$m_{NO,comp}(T_{soil}, WFPS)=\frac{P(T_{soil,}WFPS)}{k(T_{soil}, WFPS)} \times \left(\frac{V_m}{M_N} \times 10^3\right) \quad (12)$$

In Eq. (5) the last term considers the $m_{NO,comp}$ and the ambient NO concentration, however it has to be stated that the $m_{NO,comp}$ has been found to be much larger (60–90 ppb, see Sect. 4.4.2) than the ambient NO mixing ratio in the Kalahari region (<0.8 ppb, see Sect. 4.4.1).

2.7 Error estimation of NO release measurements

To determine the detection limit of our J release measurements, inert glass beads and autoclaved soils were used to measure the "blank" net release of NO as shown in the study of Feig et al. (2008). It was found that the "blank" net release of NO from the glass beads was at a rate of 0.02 ng kg^{-1} s^{-1}, with a random deviation of 0.02 ng kg^{-1} s^{-1} irrespective of the moisture content, therefore an experimentally derived detection limit for J_{NO} of 0.08 ng kg^{-1} s^{-1} may be considered. This results from the mean release rate of glass beads plus 3 standard deviations (corresponding to a confidence interval of 99.7%). Similarly, the detection limit of the autoclaved soils is 0.11 ng kg^{-1} s^{-1}, therefore the more conservative estimate from the autoclaved soils was used as our detection limit.

To quantify the precision of J_{NO} measurements, the NO net release rate was determined experimentally through the simultaneous measurement of four replicates across the full range of soil moisture. The mean standard deviation on the NO net release rate was found to be 0.03 ng kg^{-1} s^{-1} irrespective of WFPS; this is lower than the experimentally derived detection limit of J_{NO}. We consider ±0.05 ng kg^{-1} s^{-1} as a conservative estimate of the experimentally derived precision of J_{NO}.

BGD
5, 4621–4680, 2008

An error propagation approach was used to estimate the error in the net potential NO flux (Harris, 1995). The error in the net potential NO flux is derived from the error of mixing ratio measurements (i.e., error of the NO analyser), error in the determination of the bulk density, error in the determination of the consumption constant k, error in the calculation of the diffusion values and error in the determination of NO production values (P) (which can be assumed to be similar to those of the J release) and the error in the water vapour measurement which is mainly the WFPS measurements (see Eq. 5).

- The error in the $NO_{Headspace}$ measurements stems from the sensitivity of the NO analyser; using 37 different measurement periods (over 13 000 individual data points) during January–October 2006 the instrument noise was found to be 0.75% of the corresponding signal.
- The error in the BD calculation was determined from:
  - The error in the balance (Model, Sartorius, Göttingen, Germany) this was found to be ±0.006 g from 20 sets of measurements in a mass range of 2–1000 g. The error was determined for a mass of 150 g giving a relative error of 0.004%.
  - A maximum relative error of 5% was assumed (conservatively) for determination of the volume of the soil sample which was finally used as the error of the BD calculations.
- The error in the consumption constant k was calculated using the absolute error calculated for J (0.04 ng kg^{-1} s^{-1}) and converted to a relative error using a J release value of 3.5 ng kg^{-1} s^{-1}), this and the relative error of the NO analyser (0.75%), resulted in a relative error in k of 1.7%.
- The noise in the water vapour measurements was determined by adding water to all the cuvettes and incubating them while there was maximum evaporation. The relative error of the water vapour measurements was estimated at 0.8%.

- The relative error in the diffusion values is derived from a 0.8% relative error in the water vapour measurements and a 5% assumed error for the bulk density measurements resulting in a relative error in the diffusion values of 5.1%
- The error in P can be calculated from the errors in J, k and the $m_{NO,headspace}$ and it is found that the absolute error of P is 0.07 ng kg^{-1} s^{-1} and if a maximum P value of 3.5 ng kg^{-1} s^{-1} is assumed, this gives a relative error of 2% in P.

Propagating the errors of all these variables, results in a relative error of 4.2% of the net potential NO flux.

2.8 Statistics and analysis

Calculations and graphs have all been done in EXCEL (Microsoft®), and IGOR® Version 6.03, while statistical analysis of the soil physical and chemical properties was done using a 2 way ANOVA after checking for normality; all statistics were done using SPSS version 16.

2.9 Up-scaling to the regional level using remote sensing and GIS techniques

The calculated net potential NO flux values (as a function of soil moisture and temperature, see Eq. 11) were used to create a regional estimate of the NO flux ($F_{up-scaled}$) under a GIS framework. To do this, three tools were developed for the use of remote sensing information. These were the following classification schemes of:

- Land use (vegetation patch);
- Soil temperature;
- Soil moisture.

All charts have been produced with a projection of UTM zone 34 (south) Spheroid WGS84 Datum WGS 84.

BGD
5, 4621–4680, 2008

2.9.1 Land use classification

The region where up-scaled NO emissions were calculated is around the town of Tsabong in the southern part of the Kalahari. Up-scaling has been limited to an area the size of a Landsat image (185 km×185 km, see highlighted square in Fig. 1). This is in the region where the field sampling took place and where the climate and soil properties are fairly homogeneous (Fig. 1). The four corners demarcating the region are (24°57′18.51″ S, 21°36′20.12″ E), (25°02′20.31″ S, 23°04′54.75″ E); (26°26′58.27″ S, 21°34′57.92″ E) and (26°30′04.40″ S, 23°05′29.43″ E). The land use for the area was described using high resolution Landsat images in combination with visual interpretation of field conditions.

Multiband Landsat images for May 2000 (Landsat-7 Enhanced Thematic Mapper), positioned within Landsat path 174 row 78, were provided by the US Geological Survey (USGS) (since this is a remote rural region it was assumed that there have be no significant changes in the land use between May 2000 and May 2006). These images were rectified to UTM zone 34 S and image processing was performed using ERDAS Imagine, version 8.7.

Vegetation cover was defined using Normalized Difference Vegetation Index (NDVI) based vegetation rendering since it provides a good spectral characterization parameter (Roettger, 2007). The NDVI was calculated using Landsat channels 3 (R: red) and 4 (IR: near infrared) using equation 13:

$$\mathrm{NDVI} = \frac{\mathrm{IR} - \mathrm{R}}{\mathrm{IR} + \mathrm{R}} \tag{13}$$

The NDVI values range from −1 to +1 and correlate with the vegetation cover; high NDVI values indicate higher biomass (Roettger, 2007) and larger plants, therefore larger vegetation (trees and shrubs) will have a higher NDVI value, while sparse vegetation and grass have lower values. Bare soil and rocks reflect in the near infrared range and therefore have NDVI values near zero, very dry soil has a negative NDVI; water, snow and clouds and reflect in the near infrared and red wavelengths and there-

BGD
5, 4621–4680, 2008

fore have values below zero; however snow and standing water is not expected in this area.

Our classification scheme for the land use was based on the NDVI pixel value and on the "supervised classification approach", where an analyst selects "training areas" that are spectrally representative of the land cover classes of interest (ERDAS Field Guide by Leica, 2005). In this case the training areas were the vegetation patches chosen at the Berry Bush Farm where the soil samples were taken (three replicates per vegetation patch type). The vegetation patches were delineated in the field with a hand held GPS device. Parametric signatures ware developed from the NDVI values of the pixels in each vegetation patch, based on statistical parameters (maximum, minimum, mean and covariance of the NDVI matrix) of the pixels that are in the training areas at a resolution of 28 m×28 m (which is smaller than the size of the vegetation patches measured in the field) (Roettger, 2007).

In this study NDVI values ranged from 0.29 to 0.00, which corresponds to "light to sparse vegetation cover and bare soils" (Roettger, 2007).

NDVI signatures for each of the patches were defined as 0.0–0.039 for the Pan, 0.040–0.057 for the Annual Grassland, 0.058–0.24 for the Perennial Grassland, and 0.25–0.29 for the Encroachment.

The land use distribution in this part of the Kalahari was later used for estimating the emissions of NO from the soil using MODIS land surface temperature data (LST). This data is provided at a coarser resolution (1 km×1 km) and it was therefore necessary to change the resolution of the land cover data from 28 m×28 m (Fig. 7a) to that of the LST (1 km× 1 km) (Fig. 7b), this up-scaling procedure was performed in GIS mapping, where one can accurately estimate block estimates from pixels of smaller resolution.

2.9.2 Soil moisture classification

The soil moisture content for the region (December 2005–November 2006) was obtained from the "Soil Moisture for Hydrometeorologic Applications in the SADC region" (SHARE) program, which is a European Space Agency project for the characterisation

of soil moisture at a 1 km resolution. The project uses the ENVISAT ASAR (Advanced synthetic aperture radar) sensor in the global mode, in conjunction METOP scaterometer sensors (Wagner et al., 2008, 2007). The spatial resolution of the SHARE soil moisture data is less than 1 km and the pixel size is 420 m (aggregated to 1×1 km). The temporal resolution is variable and the satellite generally makes a pass every 3–5 days. Here the spatial distribution of soil moisture (in terms of soil Water Filled Pore Space) is mapped using GIS techniques.

2.9.3 Soil temperature classification

Soil surface temperature was obtained from the MODIS (Moderate Resolution Imaging Spectroradiometer) land surface temperature products MOD11A2 Eight-Day LST, distributed by the Land Process Distributed Active Archive Centre (LP DAAC) for the period December 2005–November 2006. Land surface temperatures (LST) (corresponding to a skin temperature) were obtained using the "screened for cloud effects and split-windows algorithm" (Wan et al., 2002), and the day/night algorithm which is usually applied to tropical regions (Wan, 2003). The MOD11A2 Eight-day LST is the average land surface temperature over an 8 day period obtained from daily products from the MOD11A1 at a 1 km spatial resolution. The land surface temperatures were mapped for the study area using ENVI 3.6 software. Comparisons of the satellite derived surface temperatures were compared with measured soil temperatures (5 depth) at the WMO weather station at Tsabong obtained from the National Climate Data Centre (NCDC) of the National Oceanic and Atmospheric Administration (NOAA).

2.9.4 NO up-scaling

The emission of NO from the soil was calculated for 12 months based on the parameters obtained from the laboratory flux measurements, distribution of the vegetation patches obtained from Landsat, the soil moisture estimations obtained from the ENVSAT ASAR data and from the MODIS land surface temperature data, using the algo-

rithm of Meixner and Yang (2006) (see Eq. 11).

3 Results

3.1 Soil physical and chemical properties

The soils in all the vegetation patches have a high sand content of over 70% and the soils are classified as sandy loam soils, except for the Pan soils which are sandy clay loam soils. The mean bulk density of the soils is between 1.4×10^3 kg m^{-3} and 1.5×10^3 kg m^{-3} and does not differ significantly between the vegetation patches.

The mean pH in the Annual Grassland, Perennial Grassland and Encroachment patches ranges from 6.1–6.5 and does not differ significantly ($p>0.05$). However in the Pan the mean pH is 8.5 and this is significantly higher than in the other patches ($p<0.05$). Differences occur within the Pan patch where the Tree cover has a significantly lower pH than the Open. The pH values are 8.4 and 8.6 for the Tree cover and Open, respectively ($p<0.05$, $n=3$).

There are no significant differences in the mean total N contents between the vegetation patches, which range from 0.05–0.07% total N; however there are vegetation cover type related differences (Table 2). In the Encroachment and Perennial Grassland patches where the total N content under Tree cover is significantly higher than under the Open or Grass cover classes ($p<0.01$, $n=3$). There are no significant differences ($p>0.05$) in the total N continents within either the Pan or the Annual Grassland vegetation patches. The total C content of the soil does not differ between the vegetation patches; however differences occur between the vegetation cover units within the patches (Table 2). In the Encroachment patches total C is significantly higher under the Tree cover than under either the Open or Grass cover classes ($p<0.05$, $n=3$). In the Perennial Grassland the total C content under the Tree canopies is significantly higher than under the Grass or Open cover types ($p<0.05$, $n=3$). In the Annual Grassland patch the total C content under Tree cover is significantly higher than under Open

(p<0.05, n=3) and is greater than under Grass cover at the 10% confidence interval (p<0.1, n=3). In the Pan patches the soil C content is significantly higher under the Tree canopy than under the Open or Crust cover types (p<0.05, n=3) and is greater than the Grass cover type (p<0.1, n=3).

3.2 Vegetation cover

There are distinct differences in the vegetation cover patterns between the four chosen vegetation patch types.

The Annual Grassland patch was covered by 56% annual grass species, mostly *Schmiditia kalihariensis* (Stent). None of the other vegetation patches had a cover of annual grass species as high as the Annual Grassland, the Pan had the next highest cover with 14% annual grass cover.

In the Encroachment patch the vegetation cover was dominated by tree cover, almost exclusively *A. mellifera* subsp. *detinens* (Burch.), which made up 37% of the total vegetation cover in the Encroached patch, more than double the 7–15% tree cover in the other patches. The dominant vegetation types in the Perennial Grassland patches were perennial grass species, which made up 25% of the vegetation cover. In the Pan the vegetation composition was fairly evenly distributed between the vegetation functional types, however this was the only patch where 2nd or 3rd degree soil crusts made an important contribution to the vegetation cover. In all the vegetation patches there was a large amount of uncovered soil which ranged from 17% in the Annual Grassland to 45% in the Perennial Grassland.

3.3 Laboratory NO flux

Figure 3 shows an example of the net NO release (J release) values from soils of the Annual Grassland patch and under Grass cover with NO free air incubation, J release under incubation with air containing 58 ppb NO, and the calculated net potential NO flux (F_{Lab}). Under elevated NO headspace conditions the release of NO is reduced

BGD
5, 4621–4680, 2008

indicating that uptake of NO is occurring in the soil, while the shapes of the emission curves are comparable. The flux of NO has slightly differing optimal soil moisture to the two release values due to the position of the areas of NO uptake.

In all the vegetation patches the maximum net potential NO flux was below 5 ng m^{-2} s^{-1} (Fig. 4). The highest net potential NO fluxes occurred from the soils in the Perennial Grassland and Encroachment patches, 4.3 ng m^{-2} s^{-1} (25°C), 3.1 ng m^{-2} s^{-1} (35°C) in the Perennial Grassland, 3.3 ng m^{-2} s^{-1} (25°C) and 3.3 ng m^{-2} s^{-1} (35°C) in the Encroachment Patch. The lowest net potential NO fluxes occurred from the Pan where the NO flux did not exceed 0.6 ng m^{-2} s^{-1} and 1.3 ng m^{-2} s^{-1} at 25°C and 35°C, respectively. This indicates that there are differences between the vegetation patches, caused either by the soil physical properties or by the differing vegetation.

In all the patches, except the Perennial Grassland, the potential NO flux is greater at the 35°C incubation than the 25°C incubation. In the Perennial Grassland the potential flux was greater at 25°C, indicating that there is an optimum soil temperature for the emission of NO, above which the emissions start to decrease. There is no constant pattern as to which vegetation cover type produces the highest or lowest NO flux, as these change between the different vegetation patches and is not even consistent under the different temperature treatments. However at 25°C the maximum net potential NO flux tends to occur under the dominant vegetation cover unit within the vegetation patch.

- In the Pan patch the maximum net potential NO flux from under the Crusts (0.6 ng m^{-2} s^{-1}) is more than 25% higher than under any of the other vegetation cover units (0.4 ng m^{-2} s^{-1} for Grass and Trees and 0.3 ng m^{-2} s^{-1} for Open);
- In the Annual Grassland the maximum net potential NO flux under Grass cover (1.95 ng m^{-2} s^{-1}) is twice as high as under the highest of the other vegetation cover types (0.9 ng m^{-2} s^{-1}).;
- In the Perennial Grassland patch the maximum net potential NO flux of 4.3 ng m^{-2} s^{-1} occurs from the Open cover type, while the maximum net potential

NO flux from under Trees is 3.2 ng m^{-2} s^{-1} and 2 ng m^{-2} s^{-1} from under the Grass canopy.

– In the Encroachment patch the maximum net potential NO flux from under the Tree canopies (3.3 ng m^{-2} s^{-1}) is between 25% and 50% higher than under the Open (1.6 ng m^{-2} s^{-1}) and Grass cover (2 ng m^{-2} s^{-1}).

At 35°C these patterns have changed so that in the Annual Grassland, Perennial Grassland and Encroachment sites the maximum net potential NO flux comes from under the Trees, while in the Pan patch it occurs under the Grass canopy.

The median optimal WFPS (where F_{lab} is maximum) for all patches and covers at 25°C is 16.3% (12.4% and 20% for 25 and 75 percentile respectively). At 35°C the median optimal WFPS is slightly higher at 19.3% WFPS (14.5% and 21.9%, for the 25 and 75 percentile, respectively), although these differences are not significant (p>0.05). Therefore the optimum soil moisture for the emission of NO is fairly low (20% WFPS=5.8%Θ), as is expected since the production of NO is a result to the aerobic process of nitrification.

3.4 Mean net potential patch NO flux

To determine the mean net potential NO flux of an entire patch, the NO flux within each patch have been apportioned from the individual net potential NO fluxes from the corresponding vegetation cover types according to the total coverage of that vegetation cover type (as shown in Fig. 2). This results in mean net potential flux curves for each of the vegetation patches (Fig. 5). The lowest mean net potential NO flux still occurs in the Pan patch where the maxima are less than 0.27 ng m^{-2} s^{-1} (25°C) and 0.89 ng m^{-2} s^{-1} (35°C), respectively. The highest net potential NO flux comes from the Perennial Grassland patch where the maximum flux (2.95 ng m^{-2} s^{-1}) is reached at soil moisture content of 24% soil WFPS and a soil temperature of 25°C. In all the patches the optimal soil moisture is between 10% and 25% WFPS.

Temperature does not have a consistent influence on the optimal WFPS. In the Pan and Perennial Grassland patches the optimal soil moisture under the two incubation temperatures is approximately the same, however in the Annual Grassland the optimal WFPS is shifted towards dryer soil conditions at the higher incubation temperature and in the Encroachment it is shifted towards wetter conditions under the higher incubation temperatures. The effect of temperature is also not consistent; in the Pan and Encroachment patches an increase in temperature results in a strong increase in net potential NO flux. The Q_{10} value is 3.54 and 1.51 for the Pan and Encroachment patches respectively. However in the Annual Grassland these effects are not as strong. In the Annual Grassland the Q_{10} value is 1.07 indicating that in the 25°C to 35°C temperature range there is virtually no temperature influence on the NO flux. In the Perennial Grassland there is a negative temperature relationship in the 25°C to 35°C temperature range (Q_{10}=0.61) and as the temperature increases the NO flux decreases.

Fitting the laboratory measured net potential NO fluxes as a function of both soil moisture and temperature gives the net potential flux curves as shown in Fig. 6. Using these curves an estimate of the net potential NO flux can be made for any known soil water and temperature content.

3.5 NO compensation mixing ratio and NO consumption rate

The median NO compensation mixing ratio (25°C) as a function of soil moisture is shown in Fig. 7a. The median $m_{NO,comp}$ ranges from 61–86 ppb NO with the highest median values occurring between 20% and 25% WFPS. The lower 25 percentile range is from 35 to 63 ppb NO while the 75 percentile range is from 86 to 147 ppb NO. The $m_{NO,comp}$ does not seem to be strongly influenced by the soil moisture content (at least not in the range of soil WFPS found in this study Sect. 3.6.2).

The NO consumption rate (k) at 25°C, calculated from Eq. (3) as a function of WFPS is shown in Fig. 7b. The maximum k occurs at approximately the same WFPS as the maximum of F_{lab} (see Fig. 5), namely between 10%–25% WFPS, although the there are no marked differences in k due to the soil moisture content. The median k

BGD
5, 4621–4680, 2008

values range from 0.9×10^{-5} $m^3\,kg^{-1}\,s^{-1}$ (30%–35% WFPS) to 1.3×10^{-5} $m^3\,kg^{-1}\,s^{-1}$ (15%–20% WFPS). The lower 25 percentile ranges from 3.7×10^{-6} (55%–60% WFPS) to 9.3×10^{-6} $m^3\,kg^{-1}\,s^{-1}$ (20%–25% WFPS) and the upper 75 percentile ranges from 1.5×10^{-5} (2.5%–5% WFPS) to $3.4\times10^{-5}\times10^{-5}$ $m^3\,kg^{-1}\,s^{-1}$ (25%–30% WFPS).

3.6 NO up-scaling

Up-scaling the NO flux from the corresponding mean net potential NO flux for each of the vegetation patches (see Fig. 6) to the regional scale required three sets of landscape based information: the vegetation patch distribution; the soil moisture content; and the soil surface temperature.

3.6.1 Vegetation patch distribution

Using the Landsat NDVI (see Sect. 2.9.1) provided a high resolution distribution of the vegetation patches (28 m×28 m) in this region (Fig. 1) of the southern Kalahari (Fig. 8a). The proportion of land cover from each patch type was 60.3% for Perennial Grassland, 26.8% for Annual Grassland, 6.3% for Encroachment and 6.6% for Pan. Decreasing the resolution of the vegetation patch distribution to 1 km×1 km (Fig. 8b) did not result in any major changes in the proportion of land covered by the vegetation patches; percentage distribution was 59.9%, 26.9%, 6.4% and 6.8% for the Perennial Grassland, Annual Grassland, Encroachment and Pan respectively.

3.6.2 Soil moisture

The mean monthly soil WFPS for the up-scaled section of the southern Kalahari for the period December 2005–November 2006 (see Sect. 2.9.2) is presented in Fig. 9a. It can be seen that there is considerable spatial and temporal heterogeneity in the distribution of the soil moisture. The wettest months are January and February (austral summer) where the maximum soil moisture was found to be 71% WFPS, and the areas of high

BGD
5, 4621–4680, 2008

soil moisture are widely distributed through the region. There was also an increase in the mean soil moisture content between March and May and following rains in October, although in these time periods the soil moisture distribution is patchier and less widely distributed. The soils were driest in July where the mean WFPS in the soils was less than 20%. Spatial differences exist where small scale convective storms occurred, creating a patchy distribution of soil moisture through the landscape. These estimates are partly corroborated from gravimetric soil moisture data in a study by (Thomas et al., 2008) which occurred at the Berry Bush Farm in May 2006, which is equivalent to a soil moisture content of 22.5%–34% WFPS (10–15% volumetric soil moisture). The monthly range of the soil moisture contents can be seen in Fig. 10b, where the mean values range from 20% to 48%.

3.6.3 Soil surface temperature

The soil surface temperature for December 2005–November 2006 was obtained from the MODIS instrument at a resolution of 1 km (see Sect. 2.9.3) and is shown in Fig. 10a. Variations can be seen in the land surface temperature values (averaged over 8 days) which range from approx. 13°C in July (austral winter) to 47°C in January (austral summer). While some spatial differences occur across the landscape the spatial distribution is not as marked as those found in the soil moisture distribution. Figure 10b shows a comparison between the surface temperature obtained for the Tsabong area using the remote sensing technique and the measured mean monthly temperature measured at the Tsabong meteorological station at a depth of 5 cm. It can be seen that the remote sensing estimates follow the pattern of the measured soil temperature very closely except in the austral summer months (December –March) where the soil is somewhat cooler (1–3.4°K) at a depth of 5 cm than it is at the surface.

3.6.4 Up-scaled NO fluxes

The up-scaled NO flux for the selected part of the southern Kalahari is presented in Fig. 11a. The up-scaled mean monthly flux of NO ranges from 0–323 $g\,ha^{-1}\,month^{-1}$ (0 to 13.6 $ng\,m^{-2}\,s^{-1}$) over the course of the year. The highest emissions of NO occurred from the least disturbed of the vegetation types, the Perennial Grassland where the emissions of NO reached a maximum of 323 $g\,ha^{-1}\,month^{-1}$ in some of the pixels in February 2006, although the largest mean NO emission was 240 $g\,ha^{-1}\,month^{-1}$ (9.9 $ng\,m^{-2}vs^{-1}$) for February 2006. The next highest rate of NO emission occurred in the Encroached sites where the flux of NO reached a maximum of 143 $g\,ha^{-1}\,month^{-1}$ (5.4 $ng\,m^{-2}\,s^{-1}$) and the largest mean flux was 124 $g\,ha^{-1}\,month^{-1}$ (4.6 $ng\,m^{-2}\,s^{-1}$) in January 2006. In the Annual Grassland vegetation patches the greatest mean monthly NO flux was 119 $g\,ha^{-1}\,month^{-1}$ (2.0 $ng\,m^{-2}\,s^{-1}$) while a maximum pixel value of 216 $g\,ha^{-1}\,month^{-1}$ (3.6 $ng\,m^{-2}\,s^{-1}$) was recorded in March 2006. Mean up-scaled NO fluxes were lowest in the Pan patches and the largest mean flux was 33 $g\,ha^{-1}\,month^{-1}$ (1.4 $ng\,m^{-2}\,s^{-1}$) in February 2006 while the highest pixel value was 60 $g\,ha^{-1}\,month^{-1}$ (3.15 $ng\,m^{-2}\,s^{-1}$) which occurred in March 2006. The maximum up-scaled flux was reached in the austral summer where the greatest biogenic emissions of NO were produced in the warm, moist month of February. The lowest NO fluxes occurred in the austral winter months where the soil temperature and moisture content were at the lowest in the annual cycle. During June, July and August the flux of NO out of the soil in these ecosystems is negligible (in July 2006, the maximum NO flux was less than 1.8 $g\,ha^{-1}\,month^{-1}$).

4 Discussion

This study has tried to up-scale the emissions of NO from differing vegetation patches in an arid Kalahari savanna. During the course of the study three main aspects were focused on these were:

BGD
5, 4621–4680, 2008

1. The soil physical and chemical properties, including the soil texture, pH the total N and C contents.

2. The net potential NO flux, which was measured in the laboratory and examines both inter and intra patch differences

3. The NO flux up-scaled to a region the size of a Landsat image (185 km×185 km) using a combination of remote sensing techniques.

4.1 Soil physical and chemical properties

In this study we recorded soil textures consisting of 71–79% sand, 3.8–7.6% silt and 16.5–21% clay (see Table 1). Differences in the soil textural classes between the Pan and the other vegetation patches has been previously noticed, while soil textures of the Perennial Grassland, Encroachment and Annual Grassland are typical of the Kalahari sands. The Pan patches have more clayey soil and are more calcareous resulting in a higher pH (van Rooyen and van Rooyen, 1998).

The mean total soil C and total N values reported in this study (see Table 2) range from 0.2%–1% total C and from 0.03%–0.12% total N. These are at the lower end of values reported from the Kalahari in other studies, where the soil C ranges from 0.2% to 6% (Aranibar et al., 2004; Dougill et al., 1998; Feral et al., 2003) and the reported soil N contents range from 0.025–0.045% (Aranibar et al., 2004). Few differences in the mean soil chemical properties between the differing patches occurred, however there were differences within each of the patches.

In this study, differences in the soil chemical properties were found under differing vegetation cover units within each of the patches. In most of the vegetation patches the total soil C and total soil N were higher under tree canopies than away from the canopies. This has also been found in other studies (Dougill and Thomas, 2004; Hagos and Smit, 2005). The differences in soil nutrient concentration under the tree canopies have a number of possible causes; firstly the tree species in this region are dominated

by members of the *Mimosaceae* family all of them within the *Acacia* genus. The *Acacia* genus is known to undergo the process of biological nitrogen fixation (Dougill and Thomas, 2002; Scholes and Walker, 1993; Schulze et al., 1991). It has also been proposed that the "island of fertility effect" is due to nutrients being trapped by plant stems and root systems (Aranibar et al., 2004; Hagos and Smit, 2005; Ludwig and Tongway, 1995; Ludwig et al., 1999; Tongway et al., 1989).

The results of the soil physical and chemical investigations show that all the vegetation patches, apart from the Pan soils, can be considered to be on a fairly homogenous substrate shown by the similarity in the soil textural properties, soil pH and the total C and N contents of the soil (Aranibar et al., 2004; Scholes et al., 2002), however there are micro-scale differences in the soil physical and chemical properties due to the presence of differing vegetation cover. These micro-scale differences are what drive the variation in biological processes between the vegetation patches and as a result are likely to influence the net potential NO flux from the soil.

4.2 Net potential NO flux

This is the fifth study of the biogenic emissions of NO from soils in savanna ecosystems of southern Africa, which has been conducted using a similar laboratory technique. Other studies include:

- The Nylsvley Savanna where the flux on NO ranged from 0.12 ng m^{-2} s^{-1} to 13.86 ng m^{-2} s^{-1} with mean and median values of 2.89 ng m^{-2} s^{-1} and 0.90 ng m^{-2} s^{-1} respectively (Otter et al., 1999).
- Miombo savannas and grasslands in Zimbabwe where the NO flux ranged from 0.5 ng $^{-2}$ s^{-1} to 9.4 ng m^{-2} s^{-1} with mean and median values of 2.93 ng m^{-2} s^{-1} and 1.1 ng m^{-2} s^{-1} respectively (Kirkman et al., 2001).
- The Botswana Kalahari Transect where the values ranged from 8 ng m^{-2} s^{-1} to 60 ng m^{-2} s^{-1} with mean and median values of 27.4 ng m^{-2} s^{-1} and 21 ng m^{-2} s^{-1}

respectively (Aranibar et al., 2004).

– Landscape in the Kruger National Park in South Africa where the NO flux ranged from 0.06 ng m^{-1} s^{-1} to 3.52 ng m^{-1} s^{-1} and mean and median values were 1.67 ng m^{-2} s^{-1} and 1.63 ng m^{-2} s^{-1} respectively (Feig et al., 2008).

The net potential NO fluxes calculated for the differing vegetation patches in this study (0–3.5 ng m^{-2} s^{-1}) correspond very well with the values previously reported by Otter (1999), Kirkman (2001) and Feig (2008). The reasons why the Aranibar et al. (2004) study gave such differing results is unclear and the causes cannot currently be judged.

In other natural arid and semi-arid regions (mean annual precipitation <700 mm) the measured median NO fluxes range from 0.07 ng m^{-2} s^{-1} to 5.3 ng m^{-2} s^{-1} (with reported values of up to 83 ng m^{-2} s^{-2} occurred during a pulsing event, such as when the soil is wetted or fertilized) (Davidson et al., 1993; Feig et al., 2008; Hartley and Schlesinger, 2000; Holst et al., 2007; Martin and Asner, 2005; Martin et al., 1998; McCalley and Sparks, 2008; Smart et al., 1999). The NO fluxes from these arid and semi-arid ecosystems tend to be fairly low in comparison with some of the values reported from temperate and tropical forests where fluxes of 22 ng m^{-2} s^{-1} (Pilegaard et al., 2006) and 58 ng m^{-2} s^{-1} (Butterbach-Bahl et al., 2004) were reported in European coniferous and Australian tropical forests respectively.

4.3 Intra and inter patch variability

Within each of the vegetation patches differences in the net potential NO flux occurred under the different vegetation cover types, although the patterns were not consistent between the vegetation patches either due to the soil nutrient status or due to changes in the microclimates under differing vegetation cover types.

Once the mean net potential NO flux was determined for each of the vegetation patches (by incorporating the proportion of different cover units within each of the vegetation patch types) it could be seen that differences in the mean net potential fluxes of NO occurred between the four vegetation patches. These emissions were affected by

both the soil temperature and the soil moisture; however (like in the case of the intra-patch variability) the effect of these factors was not consistent between the vegetation patches.

The Pan patches produced the lowest mean net potential NO emissions (maximum emission less than 1 ng m^{-2} s^{-1} at 35˚C) irrespective of the soil moisture content or the soil temperature. The Pan however has different soil properties to the other patches (see Sect. 3.1) while the Perennial Grassland, Annual Grassland and Encroachment patches can be considered to occur on the same soil type, and differences in the vegetation patterns are due to changes in the disturbance regime.

In the vegetation patches that occur on the same soil substrate the maximum mean net potential NO flux was between 1.5 ng m^{-2} s^{-2} and 3.5 ng m^{-2} s^{-2}. Of these vegetation patches the lowest emissions occurred in the Annual Grasslands (This is still higher than the maximum mean net potential NO flux from the Pan) and there did not appear to be an influence of temperature at the 25˚C–35˚C range. The maximum mean net potential NO flux from the Encroachment site is higher than that of the Annual Grassland and is influenced by the soil temperature where a positive temperature relationship occurs. The highest maximum mean net potential NO flux comes from the Perennial Grassland patches, however there is a negative temperature relationship between 25˚C and 35˚C.

Changes in the emission patterns between the vegetation patches indicates that when there is an increase in disturbance, resulting in a change from undisturbed Perennial Grassland to disturbed Annual Grassland, there is a reduction in the emission of NO from the soil. However as the levels of vegetation disturbance (see Sect. 2.1) increase to the point of forming an Encroachment zone the increased nutrient content and N cycling rate that occurs under the high tree cover increases the emission of NO to levels similar to that found in the undisturbed Perennial Grassland.

While under most of the soil types there was a positive or neutral relationship between the emission of NO and the temperature, this did not occur in the Perennial Grassland soils between incubation temperatures of 25˚C to 35˚C and a negative re-

BGD
5, 4621–4680, 2008

lationship between the soil temperature and the flux of NO was found. A negative relationship between the soil temperature and the emission of NO has previously been reported in the field but this generally only occurs above very high soil temperatures (40°C) (Passianoto et al., 2004). It is interesting that in the study by (Thomas et al., 2008) at the same site, a negative relationship between the soil temperature and the emission of CO_2 was found in the Kalahari sands (which correspond to the Perennial Grassland patches of this study).

4.4 NO consumption rate (k) and the Compensation mixing ratio ($m_{NO,comp}$)

It is known that soils can both produce and consume NO, however there have been only a very few studies that have shown the uptake of NO in the soil. The uptake of NO in the soil can be described using two parameters, firstly the NO consumption rate (k) which determines the rate at which NO uptake occurs and secondly the compensation mixing ratio ($m_{NO,comp}$) which determines the ambient NO mixing ratio necessary for NO uptake to occur. Despite the fact that in the Kalahari uptake of NO is likely never to occur we would like to discuss the issue of the $m_{NO,comp}$ since there are only a few scattered reports of the k and the $m_{NO,comp}$ published.

4.4.1 NO consumption rate

The NO consumption rate values found in this study are within the (very wide) range of values reported in the literature, although they tend to be on the low side. The values reported in the literature range from 0.9×10^{-5} m^{-3} s^{-1} kg^{-1} to 500×10^{-5} m^{-3} s^{-1} kg^{-1}. To the best of our knowledge, there have only been five previous reports of k from drylands; these are: Nylsvley savanna in South Africa (Otter et al., 1999), from a semi-arid savanna in the Kruger National Park (South Africa) (Feig et al., 2008), from the Kalahari transect in Botswana (Aranibar et al., 2004), from a study in Zimbabwe (Kirkman et al., 2001), and an Egyptian soil (Saad and Conrad, 1993). The median k values found in our study ($0.9–1.3\times10^{-5}$ m^{-3} s^{-1} kg^{-1}) correspond closely to the values reported for

the Nysvley Savanna (1.3-2×10^{-5} m^{-3} s^{-1} kg^{-1}) (Otter et al., 1999) and for Zimbabwe (1.6–3.2×10^{-5} m^{-3} s^{-1} kg^{-1}) (Kirkman et al., 2001). However the values reported here are lower than those reported in the Kruger National Park (10–27×10^{-5} m^{-3} s^{-1} kg^{-1}) (Feig et al., 2008); Egypt (7.2–79×10^{-5} m^{-3} s^{-1} kg^{-1}) (Saad and Conrad, 1993) or the precipitation gradient study in the Kalahari (34–500×10^{-5} m^{-3} s^{-1} kg^{-1}) (Aranibar et al., 2004). Due to the limited number of studies that have reported the NO consumption rate in dryland ecosystems and the inconsistencies in the values reported it remains an open question as to how typical the values reported in this study are for dryland ecosystems.

4.5 Compensation mixing ratio ($m_{NO,comp}$)

The $m_{NO,comp}$ for NO varies with changing soil conditions and soil may change from acting as a source to acting as a sink (Conrad and Smith, 1995). The results of this study (mean values from 61–86 ppb) correspond very well to the values reported for other semi-arid savannas in southern Africa of which four studies have been reported (Fig. 12):

- Otter et al. (1999) reported $m_{NO,comp}$ of 157±19 ppb and 152±16 ppb from the Nylsvley Savanna in South Africa for nutrient poor and nutrient rich savannas respectively.
- Kirkman et al. (2001) reported $m_{NO,comp}$ which ranged from 5–11 ppb in the dry season in Zimbabwe and from 47–85 ppb during the wet season.
- Aranibar et al. (2004) reported $m_{NO,comp}$ of 39 ppb in the driest site of there study (Tshane) in the Botswana Kalahari Transect
- Feig et al. (2008), in a study in the Kruger National Park, South Africa, found the $m_{NO,comp}$ to be dependent on the soil moisture and the compensation mixing ratio reached a maximum of 40–70 ppb at a soil moisture content of between 10% and 25% WFPS.

BGD
5, 4621–4680, 2008

Other studies (Fig. 12) have shown $m_{NO,comp}$ of 140 ppb and 500 ppb in German forest, barley and meadow soils (Bollmann et al., 1999; Rudolph et al., 1996). The $m_{NO,comp}$ has been shown to change according to the soil temperature. Low $m_{NO,comp}$ of 50 ppb occur at soil temperatures of 7°C and a maximum of over 1000 ppb was observed at a temperature of 40°C. However in this study the results for the three soils studied were not consistent across the range of temperatures (Saad and Conrad, 1993). In a second study that examined the effect of temperature on the $m_{NO,comp}$, the highest compensation point values were observed at low and high temperatures (4°C and 35°C respectively), but all were in the range of 30–800 ppb (Gödde and Conrad, 1999). From the published results it can be seen that the $m_{NO,comp}$ show a broad range of values and differ according to soil type, incubation temperature and soil moisture at differing set points.

The calculated mean $m_{NO,comp}$ in this study are between 60 and 90 ppb, during the peak of NO emission, knowing the NO compensation point mixing ratios, the question could be tackled whether the soils in the Kalahari might ever act as a NO sink. NO uptake would only occur (see Sect. 2.6), if the ambient NO mixing ratio is higher than the $m_{NO,comp}$, therefore the ambient NO concentration would need to be greater than about 5 ppb for NO uptake to occur (using values above the 10 percentile range see Fig. 7a). However, even an ambient NO mixing ratio of 5 ppb would be exceptionally high for such a remote location. Unfortunately, there are no measured data of ambient NO mixing ratio from the Kalahari available. However, for comparable southern African sites, like Marondera in Zimbabwe, NO mixing ratios of 0.15–0.3 ppb have been reported (Meixner et al., 1997); aircraft measurements in the atmospheric boundary layer over northern Namibia revealed NO mixing ratios well below 0.5 ppb, even under conditions of high biogenic soil emissions (approx. 30 ng m^{-2} s^{-1}, Harris et al., 1996). Using the Max Planck Institute for Chemistry Atmospheric Chemistry Model MESSy ("Modular Earth Sub-model System", Jockel et al., 2005), it was found that the modelled surface NO mixing ratio never exceeded 0.84 ppb, and that the mean NO mixing ratio was 0.024 ppb for the period January 2000–October 2005. It is therefore highly unlikely that

BGD
5, 4621–4680, 2008

the ambient NO mixing ratio has exceeded the $m_{NO,comp}$ during 2006. The only chance that ambient NO mixing ratios may become high enough to allow for uptake of NO in the soil could occur are during biomass burning events where the NO mixing ratios in the biomass burning plume of semi arid savannas in South Africa range from 20–185 ppb (Hobbs et al., 2003; Yokelson et al., 2003). However generally the standing biomass in this region in the Kalahari is low and the fire return frequency infrequent. Considering the remoteness of the Kalahari region and the low ambient N mixing ratios occurring there, it can be expected that the soils of the Kalahari region are continuously acting as a biogenic NO source and not as a sink.

4.6 Up-scaled NO fluxes

Up-scaling of the emission of NO from differing vegetation patches in the Kalahari was made using patch mean net potential NO emissions (as a function of the soil moisture and the soil temperature) and remote sensing techniques to estimate the regional soil moisture and temperature at a 1 km*times*1 km scale for the year December 2005 to November 2006. It was found that the up-scaled NO emissions for a 185 km ×185 km area around Tsabong (see Fig. 1) differed according to the vegetation type, and according to the season. When the mean flux of NO for the entire up-scaled region was calculated it was found that the highest monthly NO flux was 167 g ha^{-1} month^{-1} which occurred in February 2006, while the lowest mean monthly fluxes totalled 0.5 g ha^{-1} month^{-1} in July. Yearly emissions of NO from the soil for 2006 totalled 0.54 kg ha^{-1} yr^{-1}.

Four laboratory based measurements, similar to the method used in this study, have been made in southern Africa, these include studies in Nylsvley Savanna (Otter et al., 1999), in Zimbabwe (Kirkman et al., 2001) in the Kruger National Park, South Africa (Feig et al., 2008). In the Nylsvley Savanna in South Africa the NO flux ranged from 1.4–1.6 kg ha^{-1} yr^{-1} (Otter et al., 1999). For the study at Marondera (Zimbabwe) the NO flux ranged from 0.9 kg ha^{-1} yr^{-1} to 1.2 kg ha^{-1} yr^{-1} (Kirkman et al., 2001). In the study in the Kruger National Park, Feig et al. (2008) reported yearly NO emissions

BGD
5, 4621–4680, 2008

of between 0.2 and 0.8 kg ha^{-1} yr^{-1}. A further study that up-scaled the annual NO mission from field measurements gave estimates of 2.1 kg ha^{-1} yr^{-1} to 2.7 kg ha^{-1} yr^{-1} for a semi-arid savanna in South Africa (Scholes et al., 2003). Therefore in comparison with other studies in Southern Africa the results are comparable. The estimated up-scaled emission of NO from the field shows distinct seasonal differences, in the austral winter the soil temperature and the soil moisture content is lower than the optimum for the production of NO, this results in low NO fluxes from the soil. In January and February (the austral summer) the soil temperatures are higher (approximately 40°C) and it is the period of the year when rain occurs, the combination of warm soils and the availability of water allow the biogenic processes that result in the formation of NO to proceed optimally. The seasonal pattern with regards to the emission of NO from the soil has been previously shown in the Nylsvley study (Otter et al., 1999) where the peak NO emissions seem in February and March. In the Zimbabwe study the period of peak NO emission is December (Kirkman et al., 2001). In both previous studies negligible NO emissions occur in the austral winter months.

The other major source of NO in African savanna ecosystems is pyrogenic emissions is from biomass burning. A number of estimates of the total emission of NO from African savannas have been made these include values of 1.04 Tg yr^{-1} (Scholes and Scholes, 1998), 4.2 Tg yr^{-1} (Sinha et al., 2003) and 3.6 Tg yr^{-1} (Andreae, 1997). If the area of savannas burnt in Africa on a yearly basis is assumed to be 440 million ha (Hao et al., 1996), the pyrogenic emission of NO ranges from 2.4–9.5 kg ha^{-1} yr^{-1}. The pyrogenic emission of NO from African savannas (2.4–9.5 kg ha^{-1} yr^{-1}) is therefore higher but still comparable to the biogenic emission of NO (0.2–2.4 kg ha^{-1} yr^{-1}). If one then looks at the timing of the two main types of NO emission, pyrogenic emissions occur predominantly in the austral winter (July–September), while the biogenic emissions occur in the austral summer (January–March see Fig. 11b).

The input of N into this region is largely from two sources, the deposition of N from the atmosphere and the biological fixation of N by vegetation and soil crusts. The estimated N deposition into savanna regions in Southern Africa ranges from 2.5–21.6 kg ha^{-1} yr^{-1}

BGD
5, 4621–4680, 2008

(Bootsma et al., 1996; Feig et al., 2007; Garstang et al., 1998; Mphepya et al., 2004; Scholes and Walker, 1993). Nitrogen input into the southern African savanna ecosystems through biological fixation has been estimated by Scholes et al. (2003) and is thought to range from 4.8 kg ha^{-1} yr^{-1} to 21 kg ha^{-1} yr^{-1} (approximately the same range as atmospheric deposition). Therefore the loss of N in the form of NO through biogenic gaseous emissions can be significant (1.3%–7.4% of the combined atmospheric and biological N fixation inputs) and biogenic emissions of NO from the soil can be considered to be an important pathway of N loss in the region.

5 Conclusions

This study has shown the usefulness of combining laboratory measurements and remote sensing data of soil moisture and temperature in the estimation of biogenic nitric oxide emissions on a regional scale; since it can incorporate heterogeneity in both the spatial and temporal scale with a fine resolution of 1 km by 1 km. This is a particularly useful technique for remote areas, structurally heterogeneous regions or developing countries where a network of ground based measuring stations does not exist, or can not be implemented.

Differences in the emission of NO occur at the individual plant and the vegetation patch scales. The lowest mean net potential NO emissions were recorded in the Pan patches and the highest emission of NO occurred from the Perennial Grassland vegetation patches. These emissions are controlled by the soil moisture status and the soil temperature. The vegetation cover of the Kalahari is structurally heterogeneous and changes in the vegetation dynamics as a result of anthropogenic activity or climate are likely to have an important effect on the biogenic production of NO.

The Kalahari has the potential for producing fairly high emissions of nitric oxide, particularly after periods of rainfall in the hot austral summer months, although in the dry austral winter period the emissions are negligible. This results in mean monthly emissions ranging from 0.6 g ha^{-1} month^{-1} (Pan in July) to 240 g ha^{-1} month^{-1} (Perennial

Grassland in February) and mean annual emissions for the period December 2005 to November 2006 of 538 g ha^{-1} for the region that we studied. The total annual emission of NO results in a loss of N from the system of between 2.5%–22% of the amount of N entering the system due to deposition from the atmosphere. The annual biogenic emissions of NO are within the same order of magnitude as the pyrogenic NO emissions (2% to 100%) and therefore are likely to play an important role in the production of ozone in the troposphere.

An analysis of the compensation point mixing ratio in this region of the Kalahari suggests that the uptake of NO into the soil will only occur under ambient NO mixing ratios greater than 10 ppb, ambient NO mixing ratios of this magnitude are highly unlikely as it is expected that they will not exceed 1ppb in this region and therefore the soils of the Kalahari will act a source of biogenic NO to the atmosphere.

Acknowledgements. This paper is dedicated to the memory of Keith Thomas of Berry Bush Farm who passed away in 2006.

The authors would like to thank; the DAAD and the Max Planck Society for providing funding which made this study possible, we would like to thank Mrs. Feyerherd for help with the production of the figures. Our thanks go to A. Thomas and A. Dougill for allowing us to use their research site.

This Open Access Publication is financed by the Max Planck Society.

References

Anderson, J. M. and Ingram, J. S. I.: Tropical Soil Biology and Fertility, A Handbook of Methods, CAB International, Wallingford, 1993.

Andreae, M. O.: Emissions of trace gases and aerosols from southern African savanna fires, in: Fire in southern African savannas ecological and atmospheric perspectives, edited by: Van Wilgen, B. W., Andreae, M. O., Goldammer, J. G., and Lindesay, J. A., Witwatersrand University Press, Johannesburg, 161–180, 1997.

Aranibar, J. N., Otter, L. B., Macko, S. A., Feral, C. J. W., Epstein, H. E., Dowty, P. R., Eckardt, F. D., Shugart, H. H., and Swap, R. J. : Nitrogen cycling in the soil-plant system along a precipitation gradient in the Kalahari sands, Global Change Biol., 10, 359–373, 2004.

Barger, N. N., Belnap, J., Ojima, D. S., and Mosier, A. R.: NO gas loss from biologically crusted soils in Canyonlands National Park, Utah, Biogeochemistry, 75, 373–391, 2005.

Bollmann, A., Koschorreck, M., Meuser, K., and Conrad, R.: Comparison of two different methods to measure nitric oxide turnover in soils, Biol. Fert. Soils, 29(1), 104–110, 1999.

Bootsma, H. A., Bootsma, M. J., and Hecky, R. E. : The chemical composition of precipitation and its significance to the nutrient budget of Lake Malawi, in: The limnology, climatology and paleoclimatology of the east African lakes, edited by: Johnson, T. C and Odada, E. O., Gordon and Breach Publishers, Australia, 251–265, 1996.

Brümmer, C., Brüggemann, N., Butterbach-Bahl, K., Falk, U., Szarzynski, J., Vielhauer, K., Wassmann, R., and Papen, H.: Soil-Atmosphere Exchange of N_2O and NO in Near-Natural Savanna and Agricultural Land in Burkina Faso (W.Africa), Ecosystems, 11(4), 582–600, 2008.

Butterbach-Bahl, K., Kock, M., Willibald, G., Hewett, B., Buhagiar, S., Papen, H., and Kiese, R.: Temporal variations of fluxes of NO, NO_2, N_2O, CO_2 and CH_4 in a tropical rainforest ecosystem, Global Biogeochem. Cy., 18, GB3012, doi:10.1029/2004GB002243, 2004.

Chameides, W. L., Fehsenfeld, F., Rodgers, M. O., Cardelino, C., Martinez, J., Parrish, D., Lonneman, W., Lawson, D. R., Rasmussen, R. A., Zimmerman, P., J., Greenberg, Middleton, P., and Wang, T.: Ozone precursor relationships in the ambient atmosphere, J. Geophys. Res., 92, 6037–6055, 1992.

Conrad, R.: Compensation concentration as critical variable for regulating the flux of trace gases between soil and atmosphere, Biogeochemistry, 27, 155–170, 1994.

Conrad, R.: Soil Microorganisms as controllers of atmospheric trace gases (H_2, CO, CH_4, N_2O

and NO), Microbiol. Rev., 60(4), 609–640, 1996.
Conrad, R. and Smith, K. A.: Soil Microbial Processes and the cycling of Atmospheric Trace Gases (and discussion), Philosophical Transactions: Physical Science and Engineering, 351(1696), 219–230, 1995.
Crutzen, P. J.: Overview of tropospheric chemistry: Developments during the past quarter century and a look ahead, Faraday Discuss, 100, 1–21, 1995.
Crutzen, P. J. and J. Lelieveld, Human impacts on atmospheric chemistry, Annu. Rev. Earth Pl. Sc., 29, 17–45, 2001.
Davidson, E. A.: Fluxes of nitrous oxide and nitric oxide from terrestrial ecosystems, in: Microbial production and consumption of Greenhouse Gases: Methane, Nitrogen Oxides and Halomethanes, edited by: Rogers, J. E. and Whitman, W. B., American Society for Microbiology, Washington D.C., 219–235, 1991a.
Davidson, E. A.: Soil Water content and the ratio of nitrous oxide to nitric oxide emitted from soil, in: Tenth International symposium on environmental biogeochemistry, Chapman and Hall, San Francisco, 369–386, 1991b.
Davidson, E. A. and Kingerlee, W.: A global inventory of nitric oxide emissions from soils, Nutr. Cycl. Agroecosys., 48, 37–50, 1997.
Davidson, E. A., Matson P. A.,Vitousek, P. M. , Riley, R., Dunkin, D., Garcia-Mendez, G., and Maass, J. M.: Processes regulating soil emissions of NO and N_2O in a seasonally dry tropical forest, Ecology, 74(1), 130–139, 1993.
Day, P. R.: Particle fractionation and particle-size analysis, in: Methods of soil analysis Part 1: Physical and mineralogical properties, including statistics of measurements and sampling, edited by: Black, C. A., Evens, D. D., Ensminge, L. E., White, J. L., and Clark, F. E., American Society of Agronomy, Madison, 545–567, 1969.
Delon, C., Serca, D., Boissard, C., Dupont, R., Dutot, A.,Laville, P. , De Rosnay, P., and Delmas, R.: Soil NO Emissions modelling using artificial neural network, Tellus, 59B, 502–513, 2007.
Denman, K. L., Brasseur, G. P., Chidthaisong, A., Ciais, P., Cox, P. M., Dickinson, R. E., Hauglustaine, D., Heinze, C., Holland, E. A., Jacob, D. J., Lohmann, U., Ramachandran, S., da Silva Dias, P. L.,Wofsy, S. C., and Zhang, X.: Couplings between changes in the climate system and biogeochemistry, in: Climate Change 2007: The physical science basis, Contribution of working group 1 to the fourth assessment report of the Intergovernmental Panel on Climate Change, edited by: Solomon, S., Qin, D., Manning, M., Chen, Z., Marquis, M., Averyt, K. B., Tignor, M., and Miller, H. L., Cambridge University Press, Cambridge,

499–588, 2007.
Dougill, A. J., Heathwaite A. L., and Thomas, D.S. G.: Soil water movement and nutrient cycling in semi-arid rangeland: vegetation change and system resilience, Hydrol. Process., 12(3), 443–459, 1998.
Dougill, A. J. and Thomas, A. D.: Nebkha dunes in the Molopo Basin, South Africa and Botswana: formation controls and their validity as indicators of soil degradation, J. Arid. Environ., 50(3), 413–428, 2002.
Dougill, A. J. and Thomas, A. D.: Kalahari sand soils: Spatial heterogeneity, biological soil crusts and land degradation, Land Degrad. Dev., 15, 233–242, 2004.
Erickson, H., Davidson, E. A., and Keller, M.: Former land-use and tree species affect nitrogen oxide emissions from a tropical dry forest, Oecologia, 130, 297–308, 2002.
Erickson, H., Keller, M., and Davidson, E. A.: Nitrogen oxide fluxes and nitrogen cycling during post agricultural succession and forest fertilization in the humid tropics, Ecosystems, 4, 67–84, 2001.
Feig, G. T., Mamtimin, B., and Meixner, F. X.: Soil biogenic emissions of nitric oxide from a semi-arid savanna in South Africa, Biogeosciences Discuss., 5, 2795–2837, 2008, http://www.biogeosciences-discuss.net/5/2795/2008/.
Feig, G. T., Scholes, M. C., Otter, L. B., and Vanlauwe, B.: Nitrogen in Africa, in: Global Climatic Change Processes and their impact on Africa: A Synthesis, edited by: Otter, L. B., Olago, D. O., and Niang, I., East Africa Educational Publishers, Nairobi, 217–243, 2007.
Feral, C. J. W., Epstein, H. E., Otter, L. B., Aranibar, J. N., Shugart, H. H., Macko, S. A., and Ramontsho, J.: Carbon and nitrogen in the soil-plant system along rainfall and land-use gradients in southern Africa, J. Arid. Environ., 54, 327–343, 2003.
Galbally, I. E. and Johansson, C.: A model relating laboratory measurements of rates of nitric oxide production and field measurements of nitric oxide emissions from soils, J. Geophys. Res., 94, 6473–6480, 1989.
Galbally, I. E., Kirstine, W. V., Meyer, C. P., and Wang, Y. P.: Soil-Atmosphere Trace Gas Exchange in Semiarid and Arid Zones, J. Environ. Qual., 37, 599–607, 2008.
Galloway, J. N., Bekunda M. A., Cai, Z., Erisman, J. W., Freney, J., Howarth, R. W., Martinelli, L., Scholes, M. C., and Seitzinger, S. P.: A preliminary assessment of "changes in the global nitrogen cycle as a result of anthropogenic influences", International Nitrogen Initiative, 1–33, 2004.
Garrido, F., Henault, C., Gaillard, H., Perez, S., and Germon, J. C.: N_2O and NO emissions by

agricultural soils with low hydraulic potentials, Soil. Biol. Biochem., 34, 559–575, 2002.
Garstang, M., Ellery, W. N., McCarthy, T. S., Scholes M. C., Scholes R. J., Swap, R. J., and Tyson, P. D.: The contribution of aerosol- and water-borne nutrients to the functioning of the Okavango Delta ecosystem, Botswana, South African Journal of Science, 94(5), 223–229, 1998.
Gödde, M. and Conrad, R.: Simultaneous measurement of nitric oxide production and consumption in soil using a simple static incubation system, and the effect of soil water content on the contribution of nitrification, Soil Biol. Biochem., 30(4), 433–442, 1998.
Gödde, M. and Conrad, R.: Immediate and adaptational temperature effects on nitric: Oxide production and nitrous oxide release from nitrification and denitrification in two soils, Biol. Fert. Soils, 30(1–2), 33–40, 1999.
Gut, A., Blatter, A., Fahrni, M., Lehmann, B.E., Neftel, A., and Staffelbach, T.: A new membrane tube technique (METT) for continuous gas measurements in soil, Plant Soil, 198, 79–88, 1998.
Hagos, M. G. and Smit G. N.: Soil enrichment by Acacia mellifera subsp. detinens on nutrient poor sandy soil in a semi-arid southern African savanna, J. Arid Environ., 61, 47–59, 2005.
Hall, S. J. and Asner, G. P.: Biological invasion alters regional nitrogen-oxide emissions from tropical rainforests, Global Change Biol., 13(8), 2143–2160, 2007.
Hao, W. M., Ward, D., Olbu, G., and Baker S. P.: Emissions of CO_2, CO and hydrocarbons from fires in diverse African savanna ecosystems, J. Geophys. Res., 101, 23 577–23 584, 1996.
Harris, D. C.: Quantitative Chemical Analysis, Freeman, W. H. and Company, New York, 716 pp., 1995.
Harris, G. W., Weinhold F. G., and Zenker, T.: Airborne observations of strong biogenic NO_x emissions from the Namibian Savanna at the end of the dry season, J. Geophys. Res., 101, 707–712, 1996.
Hartley, A. E. and Schlesinger, W. H.: Environmental controls on nitric oxide emission from northern Chihauhaun desert soils, Biogeochemistry, 50, 279–300, 2000.
Hobbs, P. V., Sinha, P., Yokelson, R., Christian, T. J., Blake, D. R., Gao S., Kirchstetter, T. W., Novakov, T., and Pilewskie, P.: Evolution of gases and particles from a savanna fire in South Africa, J. Geophys. Res., 108(D13), SAF21, 21,Doi:10.1029/2002JD002352, 21pp. 2003.
Holst, J., Liu, C. Y., Bruggemann N., Butterbach-Bahl K., Zheng X. H., Wang Y. S., Han S. H., Yao Z. S., Yue, J., and Han, X. G.: Microbial N turnover and N-oxide (N_2O/NO/NO_2) fluxes in semi-arid grassland of Inner Mongolia, Ecosystems, 10(4), 623–634, 2007.

Hutchinson, G. L., Guenzi W. D., and Livingston G. P.: Soil water controls on aerobic soil emission of gaseous nitrogen oxides, Soil Biol. Biochem., 25(1), 1–9, 1993.
Jaegle, L., Martin, R. V., Chance, K., Steinberger, L., Kurosu, T. P., Jacob, D. J., Modi, A. I., Yoboue, V., Sigha-Nkamdou, L., and Galy-Lacaux, C.: Satellite mapping of rain-induced nitric oxide emissions from soils, J. Geophys. Res.-Earth, 109, D21310, doi:10.1029/2004JD004787, 2004.
Jockel, P., Sander,R., Kerkweg, A., Tost, H., and Lelieveld, J.: Technical note: The Modular Earth Submodel System (MESSy) – a new approach towards Earth System Modelling, Atmos. Chem. Phys., 5, 433–444, 2005, http://www.atmos-chem-phys.net/5/433/2005/.
Kirkman, G. A., Yang, W. X., and Meixner, F. X.: Biogenic nitric oxide emissions upscaling: an approach for Zimbabwe, Global Biogeochem. Cy., 15(4), 1005–1020, 2001.
Le Roux, X. and Abbadie, L.: Emission of nitrogen monoxide from African tropical ecosystems: Control of emissions by soil characteristics in humid and dry savannas of West Africa, J. Geophys. Res., 100(D11), 23 133–23 142,1995.
Levine, J. S., Winstead, E.,Parsons, D. A. B. , Scholes, M. C., Scholes, R. J., Cofer, W. R., Cahoon, D. R., and Sebacher, D. I.: Biogenic emissions of nitric oxide (NO) and nitrous oxide (N_2O) from savannas in South Africa: The impact of wetting and burning, J. Geophys. Res., 101, 23 683–23 688, 1996.
Lloyd, J. and Taylor, J. A.: On the Temperature-Dependence of Soil Respiration, Funct. Ecol., 8(3), 315–323, 1994.
Logan, J. A.: Nitrogen oxides in the troposphere: global and regional budgets, J. Geophys. Res., 88, 10 785–10 807, 1983.
Ludwig, J., Meixner, F. X., Vogel, B., and Förstner, J.: Soil-air exchange of nitric oxide: An overview of processes, environmental factors, and modelling studies, Biogeochemistry, 52, 225–257, 2001.
Ludwig, J. A. and Tongway, D. J.: Spatial organisation of landscapes and its function in semi-arid woodlands, Australia, Landscape. Ecol., 10, 51–63, 1995.
Ludwig, J. A., Tongway, D. J., and Marsden, S. G.: Stripes, strands or stipples: Modelling the influence of three landscape banding patterns on resource capture and productivity in semi-arid woodlands, Australia, Catena, 37, 257–273, 1999.
Martin, R. E. and Asner, G. P.: Regional estimate of nitric oxide emissions following woody encroachment: linking imaging spectroscopy and field studies, Ecosystems, 8, 33–47, 2005.

Martin, R. E., Asner, G. P., Ansley, R. J., and Mosier, A. R.: Effects of woody vegetation encroachment on soil nitric oxide emissions in a temperate savanna, Ecol. Appl., 13(4), 897–910, 2003a.

Martin, R. E., Scholes M. C., Mosier A. R., Ojima, D. S., Holland, E. A., and Parton, W. J.: Controls on annual emissions of nitric oxide from soils of the Colorado Shortgrass Steppe, Global Biogeochem. Cy., 12(1), 81–91, 1998.

Martin, R. V., Jacob, D. J.,Chance, K. , Kurosu, T. P., Palmer, P. I., and Evens, M. J.: Global inventory of nitrogen oxide emissions constrained by space based observation of NO_2 columns, J. Geophys. Res., 108(D17), 4437, doi:10.1029/2003JD003453, 2003b.

McCalley, C. K. and Sparks, J. P.: Controls over nitric oxide and ammonia emissions from Mojave Desert soils, Oecologia, 156(4), 871–881, 2008.

Meixner, F. X.: Surface exchange of odd nitrogen oxides, Nova Acta Leopoldina, NF 70(288), 299–348, 1994.

Meixner, Fickinger F. X., Marufu, T., Serca, L., Nathaus D., Makina F. J., Mukurumbira, E., L., and Andreae, M. O.: Preliminary results on nitric oxide emission from a southern African savanna ecosystem, Nutr. Cycl. Agroecosys., 48, 123–138, 1997.

Meixner, F. X. and Yang, W. X.: Biogenic emissions of nitric oxide and nitrous oxide from arid and semi-arid land, in: Dryland Ecohydrology, edited by: 'Odorico, P. D. Porporat, A., Springer, Dordrecht, 233–255, 2006.

Moldrup, P., Olesen, T. R., Gamst, J., Schjonning, P., Yamaguchi, T., and Rolston, D. E.: Predicting the gas diffusion coefficient in repacked soil: Water-induced linear reduction model, Soil. Sci. Soc. Am. J., 64, 1588–1594, 2000.

Monks, P. S.: Gas-phase radical chemistry in the troposphere, Chem. Soc. Rev., 34, 376–395, 2005.

Mosier, A. R., Pendal, E., and Morgan, J. A.: Effect of water addition and nitrogen fertilization on the fluxes of CH_4, CO_2, NO_x, and N_2O following 5 years of elevated CO2 in Colorado Shortgrass Steppes, Atmos. Chem. Phys., 3, 1703–1708, 2003, http://www.atmos-chem-phys.net/3/1703/2003/.

Mphepya, J. N., Pienaar, J. J., Galy-Lacaux, C., Held, G., and Turner, C. R.: Precipitation chemistry in semi-arid areas of southern Africa: A case study of a rural and an industrial site, J. Atmos. Chem., 47, 1–24, 2004.

Otter, L. B., Yang, W. X., Scholes, M. C., and Meixner, F. X. : Nitric Oxide emissions from a southern African Savanna, J. Geophys. Res., 104(D15), 18 471–18 485 1999.

Parsons, D. A. B., Scholes, M. C., Scholes, R. J., and Levine, J. S.: Biogenic NO emission from savanna soils as a function of fire regime, soil type, soil nitrogen and water status, J. Geophys. Res, 101(D19), 23 683–23 688, 1996.
Parton, W. J., Holland, E. A., Del Grosso, S. J., Hartman, M. D., Martin, R. E., Mosier, A. R., Ojima, D. S., and Schimel, D. S.: Generalized model for NO_x and N_2O emissions from soils, J. Geophys. Res, 106(D15), 17 403–17 419, 2001.
Passianoto, C. C., Ahrens, T., Feigl, B. J., Streudler, P. A., Melillo, J. M., and do Carmo, J. B.: Diurnal changes in nitric oxide emissions from conventional tillage and pasture sites in the Amazon Basin: influence of soil temperature, Plant Soil, 258, 21–29, 2004.
Pilegaard, K., Skiba, U., Ambus, P., Beier, C. , Buggemann, N., Butterbach-Bahl, K., Dick, J., Dorsey, J., Duyzer, J., Gallagher, M., Gasche, R., Horvarth, L., Kitzler, B., Leip, A., Pihlatie, M. K., Rosenkranz, P., Seufert, G., Vesala, T., Westrate, H., and Zechmeister-Boltenstern S.: Factors controlling regional differences in forest soil emission of nitrogen oxides (NO and N_2O), Biogeosciences, 3, 651–661, 2006, http://www.biogeosciences.net/3/651/2006/.
Remde, A., Slemr, F., and Conrad, R.: Microbial production and uptake of nitric oxide in soil, FEMS Microbiol. Ecol., 62, 221–230, 1989.
Ringrose, S., Matheson, W., and Vanderpost, C.: Analysis of soil organic carbon and vegetation cover trends along the Botswana Kalahari Transect, J. Arid. Environ., 38, 379–396, 1998.
Roettger, S.: NDVI-based vegetation rendering, Proceedings of the Ninth IASTED International Conference on Computer Graphics and Imaging, 41-53, 2007.
Rudolph, J. and Conrad, R.: Flux between soil and atmosphere, vertical concentration profiles in soil, and turnover of nitric oxide.2. Experiments with naturally layered soil cores, J. Atmos. Chem. , 23(3), 275–300, 1996.
Rudolph, J., Rothfuss, F., and Conrad, R.: Flux between soil and atmosphere, vertical concentration profiles in soil, and turnover of nitric oxide. 1. Measurements on a model soil core, J. Atmos. Chem., 23(3), 253–573, 1996.
Russow, R., Sich, I., and Neue, H.-U.: The formation of the trace gases NO and N_2O in soils by the coupled processes of nitrification and denitrification: results of kinetic ^{15}N tracer investigations, Chemosphere, 2, 359–366, 2000.
Saad, O. A. L. O. and Conrad R.: Temperature dependence of nitrification, denitrification and turnover of nitric oxide in different soils, Biol. Fert. Soils, 15, 21–27, 1993.
Scholes, M. C., Martin, R., Scholes, R. J., Parsons, D., and Winstead, E.: NO and N_2O emis-

sions from savanna soils following the first simulated rains of the season, Nutr. Cycl. Agroecosys., 48, 115–122, 1997.
Scholes, M. C., Scholes, R. J., Otter, L. B., and Woghiren, A. J.,: Biogeochemistry: The cycling of elements, in: The Kruger experience, ecology and management of savanna heterogeneity, edited by: Du Toit, J. T., Rogers, K. H., and Biggs, H. C., Island Press, Washington, 130–148, 2003.
Scholes, R. J., Dowty, P. R.,Caylor, K. , Parsons, D. A. B., Frost, P. G. H., and Shugart, H. H.: Trends in savanna structure and composition along an aridity gradient in the Kalahari, J. Veg. Sci., 13(3), 419–428, 2002.
Scholes, R. J. and Parsons D. A. B.: The Kalahari transect: research on global change and sustainable development in southern Africa, IGBP, Stockholm, Sweden, 63 pp., 1997.
Scholes, R. J. and Scholes, M. C.: Natural and human related sources of ozone-forming trace gases in southern Africa, S. Afr. J. Sci., 93, 1–4, 1998.
Scholes, R. J. and Walker, B. H.: An African Savanna synthesis of the Nylsvley study, Cambridge University Press, Cambridge, 306 pp., 1993.
Schulze, E. D., Gebauer, G., Ziegler, H., and Lange O. L.: Estimation of N fixation by trees on an aridity gradient in Namibia, Oecologia, 88, 451–455, 1991.
Serca, D., Delmas, R., Le Roux, X., Parsons, D. A. B., Scholes, M. C., Abbadie, L., Lensi, R., Ronce, O., and Labroue, L.: Comparison of nitrogen monoxide emissions from several African tropical ecosystems and influence of season and fire, Global Biogeochem. Cy., 12(4), 637–651, 1998.
Sinha, P., Hobbs P. V., Yokelson R., Bertschi, I. T., Blake D. R., Simpson, I. J., Gao, S., Kirchstetter, T.W., and Novakov, T. : Emissions of trace gases and particles from savanna fires in southern Africa, J. Geophys. Res.-Atmos., 108, p. 8487, 2003.
Skopp, J., Jawson, M. D., and Doran, J. W.: Steady-State Aerobic Microbial Activity as a Function of Soil-Water Content, Soil. Sci. Soc. Am. J. , 54(5), 1619–1625, 1990.
Smart, D. R., Stark, J. M., and Deigo, V.: Resource limitation to nitric oxide emissions from a sagebrush-steppe ecosystem, Biogeochemistry, 47, 63–86, 1999.
Steinkamp, J., Ganzeveld, L. N., Wilcke, W., and Lawrence, M. G.: Influence of modelled soil biogenic NO emissions on related trace gases and the atmospheric oxidizing efficiency, Atmos. Chem. Phys. Discuss., 8, 10 227–10 255, 2008, http://www.atmos-chem-phys-discuss.net/8/10227/2008/.
Thomas, A. D. and Dougill, A. J.: Spatial and temporal distribution of cyanobacterial soil crusts

in the Kalahari: Implications for soil surface properties, Geomorphology, 85(1–2), 17–29, 2007.
Thomas, A. D., Hoon, S. R., and Linton, P. E.: Carbon dioxide fluxes from cyanobacteria crusted soils in the Kalahari, Appl. Soil Ecol., 39(3), 254–263, 2008.
Tongway, D. J., Ludwig, J. A., and Whitford, W. G.: Mulga log mounds: fertile patches in the semi-arid woodlands of eastern Australia, Aust. J. Ecol., 14, 263–268, 1989.
Van Dijk, S. M., Gut, A., Kirkman, G. A., Meixner, F. X. , and Andreae M. O.: Biogenic NO emissions from forest and pasture soils: Relating laboratory studies to field measurements, J. Geophys. Res., 107(D20), LBA25-1-LBA, 11–25, 2002.
Van Oudtshorn, F.: Guide to the grasses of southern Africa, Briza Publications, Pretoria, South Africa, 301pp., 1999.
Van Rooyen, N. and van Rooyen, M. W.: Vegetation of the south-western arid Kalahari: An overview, Transactions of the Royal Society of South Africa, 53, 113–140, 1998.
Wagner, W., Pathe, C., Doubkova, M., Sabel, D., Bartsch, A., Hasenauer, S., Bloschl, G., Scipal, K., Martinez-Fernandez, J., and Low, A.: Temporal stability of soil moisture and radar backscatter observed by the advanced Synthetic Aperture Radar (ASAR), Sensors, 8(2), 1174–1197, 2008.
Wagner, W., Pathe C., Sabel D., Bartsch A., Künzer, C., and Scipal, K.: Experimental 1 km soil moisture products from ENVISAT ASAR for Southern Africa, in: ENVISAT and ERS Symposium, Montreux, Switzerland, 2007.
Wan, Z.: Land surface temperature measurement from EOS MODIS data report,National Aeronautics and Space Administration, Santa Barbara California, USA, 2003.
Wan, Z., Zhang Y. , Zhang, Q., and. Li, Z. L: Validation of the land surface temperature product retrieval from Terra Moderate Resolution Imaging Spectroradiometer Data, Remote Sens. Environ., 87, 163–180, 2002.
Yokelson, R., Bertschi, I. T., Christian, T. J., Hobbs, P. V., Ward, B. B., and Hao, W. M.: Trace gas measurements in nascent, aged, and cloud-processed smoke from African savanna fires by airborne fourier transform infrared spectroscopy (aftir), J. Geophys. Res.-Atmos., 108, p. 8478, 2003.

Table 1. Mean soil physical and chemical properties for the vegetation patches. Values in brackets indicate standard deviation (n=9 for the Annual Grassland, Encroachment and Perennial Grassland, n=12 for the Pan).

Patch	Pan	Annual Grassland	Perennial Grassland	Encroachment
Bulk Density (10^3 kg m^{-3})	1.4 (0.1)	1.5 (0.1)	1.5 (0.1)	1.5 (0.1)
Sand(%)	71.0 (1.7)	78.2 (1.7)	79.0 (0.8)	78.9 (1.0)
Silt (%)	7.6 (1.5)	4.1 (1.3)	4.5 (1.3)	3.8 (1.1)
Clay (%)	21.4 (1.3)	17.6 (1.3)	16.5 (1.0)	17.3 (0.5)
Texture Class	Sandy clay loam	Sandy Loam	Sandy Loam	Sandy Loam
pH	8.5 (0.1)	6.5 (0.5)	6.1 (0.5)	6.5 (0.3)
Total N (%)	0.07 (0.02)	0.07 (0.02)	0.05 (0.02)	0.06 (0.02)
Total C (%)	0.68 (0.2)	0.49 (0.2)	0.44 (0.2)	0.38 (0.1)

Table 2. Effect of vegetation cover unit on the soil total N and C contents values in brackets indicate the standard deviation (n=3).

Patch	Vegetation Cover Unit	Total Nitrogen (%)	Total Carbon (%)
Pan	Tree	0.093 (0.028)	0.90 (0.114)
	Open	0.057 (0.008)	0.57 (0.103)
	Grass	0.067 (0.008)	0.66 (0.117)
	Crust	0.058 (0.010)	0.58 (0.094)
Annual Grassland	Tree	0.092 (0.025)	0.72 (0.21)
	Open	0.052 (0.003)	0.35 (0.03)
	Grass	0.055 (0.018)	0.40 (0.108)
Perennial Grassland	Tree	0.065 (0.010)	0.65 (0.074)
	Open	0.037 (0.008)	0.27 (0.081)
	Grass	0.035 (0.010)	0.38 (0.129)
Encroachment	Tree	0.076 (0.006)	0.51 (0.093)
	Open	0.050 (0.005)	0.30 (0.047)
	Grass	0.043 (0.006)	0.31 (0.06)

Fig. 1. 1 Map of Botswana and surrounding countries. The area where up-scaling of the NO flux occurred is highlighted

BGD
5, 4621–4680, 2008

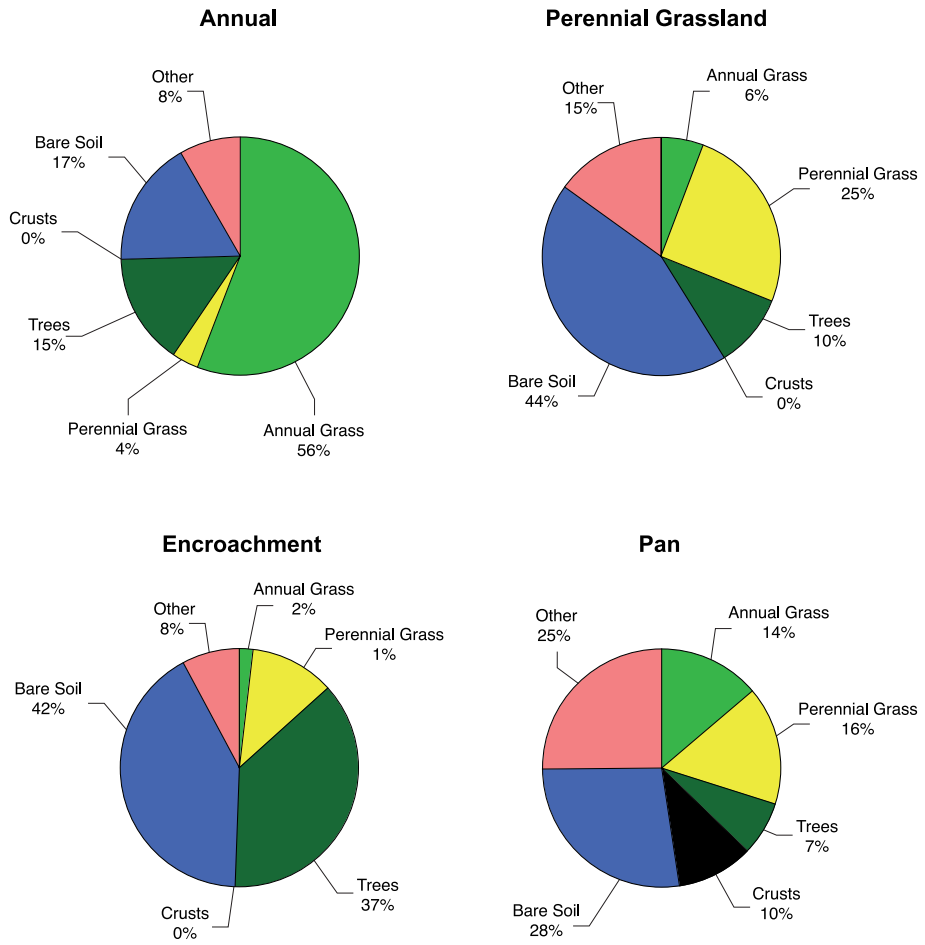

Fig. 2. Vegetation cover in each of the selected vegetation patches.

BGD
5, 4621–4680, 2008

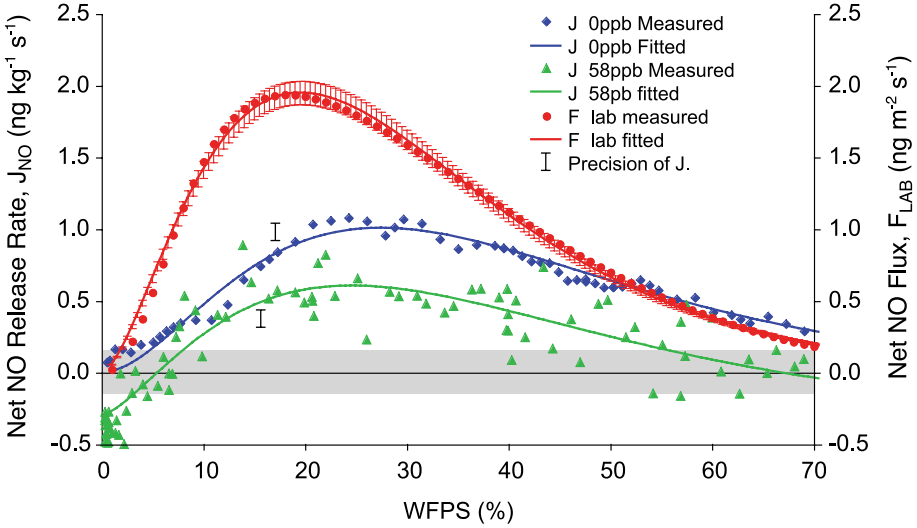

Fig. 3. An example of the measured and fitted net NO release (JNO) under low NO mixing ratios (blue), measured and fitted net NO release under high NO mixing ratios (green) and the net potential NO flux (red) for the Annual Grassland Grass cover at an incubation temperature of 25°C. Error bars indicate the precision for the *J* release measurements (0.05 ng kg^{-1} s^{-}1), while the detection limit is represented by the "dead band" (0.11 ng kg^{-1} s^{-1}) around zero net NO release rate (JNO). The error bars on the net potential NO curve represents the calculated error using a relative error of 4.2% from the error propagation approach.

BGD
5, 4621–4680, 2008

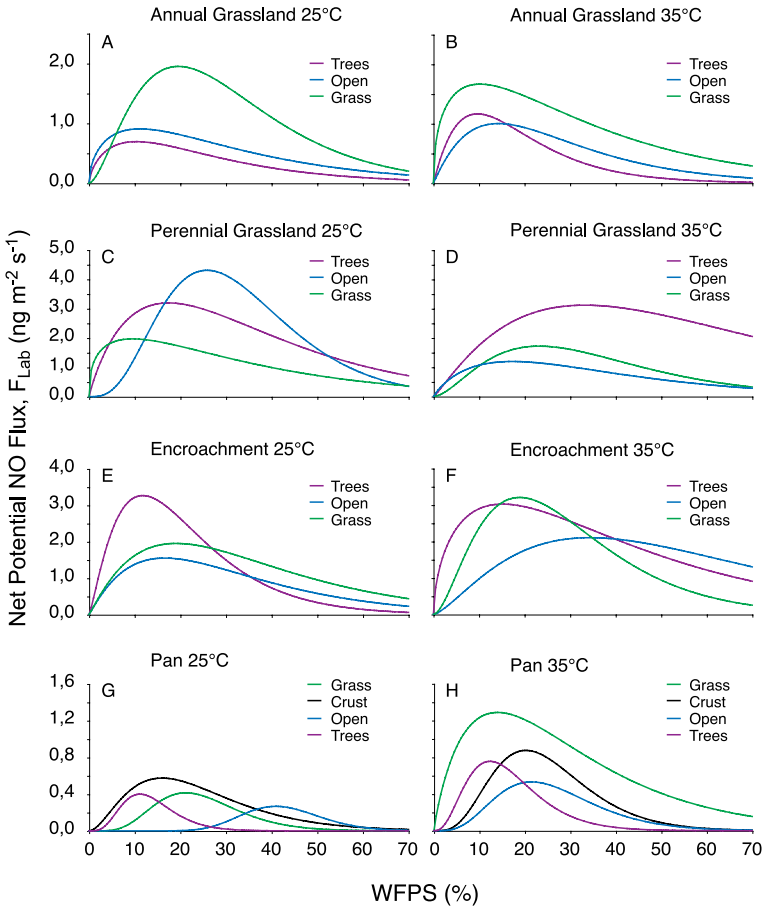

Fig. 4. Laboratory derived net potential NO flux as a function of the soil WFPS at 25° and 35° incubation temperatures.

BGD
5, 4621–4680, 2008

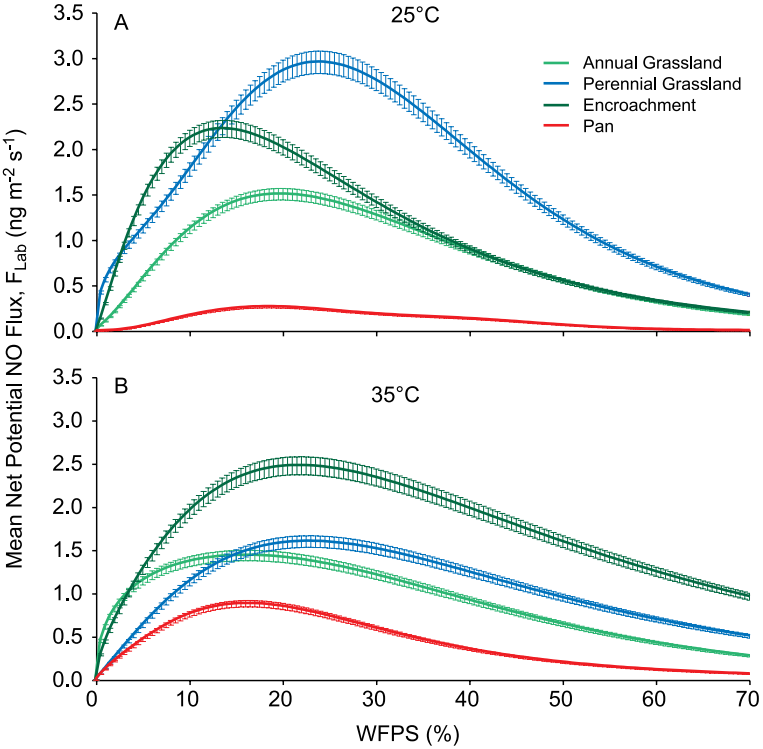

Fig. 5. (A) Mean net potential NO flux at 25° incubation. **(B)** Mean net potential NO flux at 35°. Error bars represent the 4.2% relative uncertainty determined for the NO flux (Sect. 2.7). The mean net potential NO flux is determined in each of the vegetation patches taking into account the proportion of vegetation cover (see Fig. 2).

BGD
5, 4621–4680, 2008

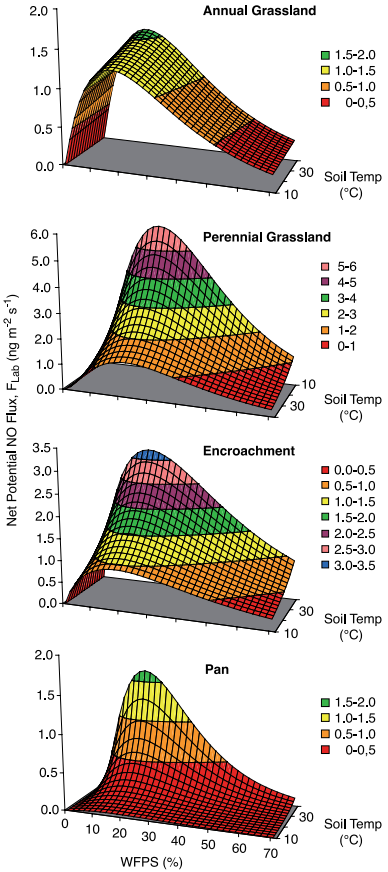

Fig. 6. Mean net potential NO flux charts for each of the four vegetation patches as a function of both soil moisture (in terms of WFPS) and soil temperature. Note that the temperature scale in the Perennial Grassland figure is reversed and in fact shows negative temperature dependence.

BGD
5, 4621–4680, 2008

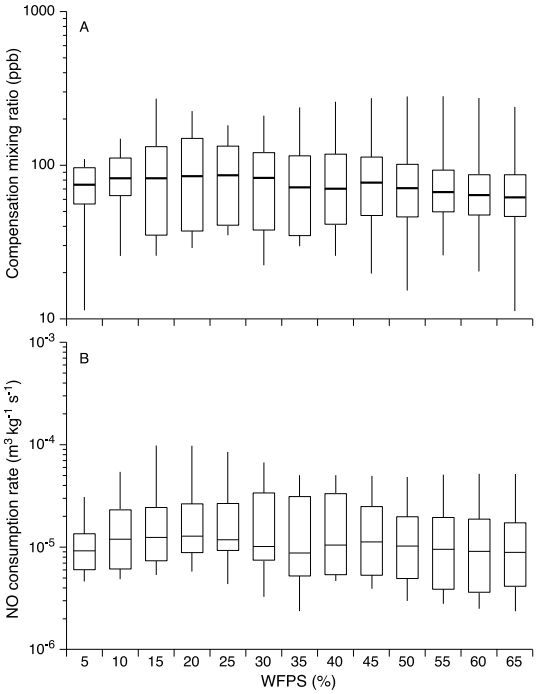

Fig. 7. (A) Median $m_{NO,comp}$ at 25°C for all the soils grouped into soil WFPS intervals of 5% WFPS for the range of WFPS that occurred in the field. The bar indicates the median $m_{NO,comp}$ while the box and whiskers indicate the 10, 25, 75 and 90 percentile range. **(B)** NO consumption rate at 25°, medians and percentiles for all the soil samples, the bar indicates the median k value, the box delineates the 25 percentile to the 75 percentile and the whiskers show the 10 percentile to 90 percentile range.

BGD
5, 4621–4680, 2008

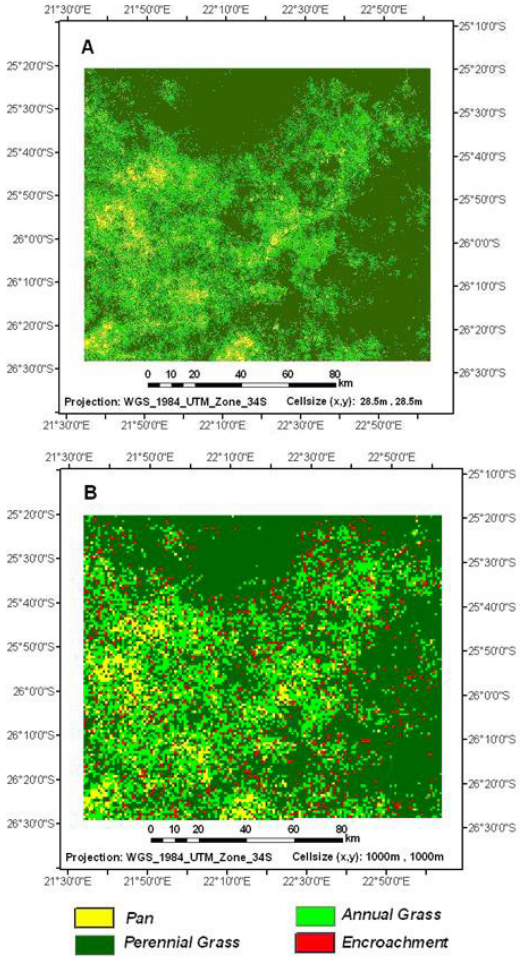

Fig. 8. (A) Land cover classification at a pixel resolution of 28 m×28 m **(B)**. Land cover classification at a resolution of 1 km×1 km.

BGD
5, 4621–4680, 2008

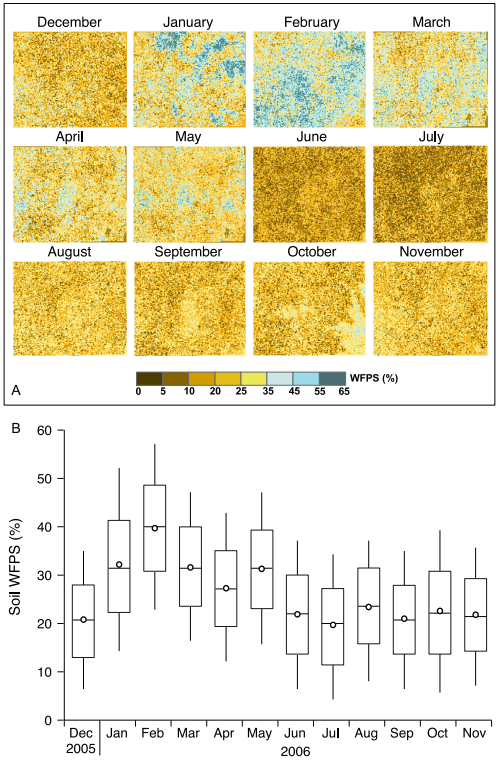

Fig. 9. **(A)** Soil moisture classification for the period December 2005 to November 2006 in terms of Soil Water Filled Pore Space (WFPS), resolution 1 km. These figs. occupy exactly the same area and are at the same resolution as Fig. 8. **(B)** monthly mean soil moisture (WFPS) for December 2005– November 2006 from the SHARE satellite data for the research area (see Fig. 9), circles represent the mean WFPS across the individual pixels, the bar in the middle of the box represents the median WFPS, the box indicates the 25 and 75 percentiles and the whiskers represent the 10 and 90 percentile.

BGD
5, 4621–4680, 2008

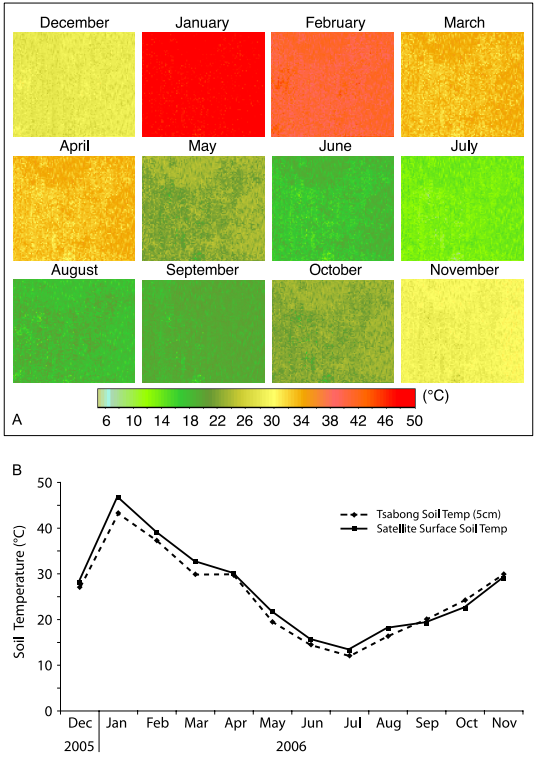

Fig. 10. **(A)** Monthly mean soil surface temperatures for the selected site (see Fig. 9) (December 2005–November 2006) **(B)** Comparison between the measured soil temperature (at 5 cm depth) at the WMO station in Tsabong and the satellite derived surface temperature (at a 1 km×1 km scale) for the pixel including the Tsabong WMO station for the period December 2005–November 2006. Deviations between the satellite and measured values arise from the depth of measurement.

BGD
5, 4621–4680, 2008

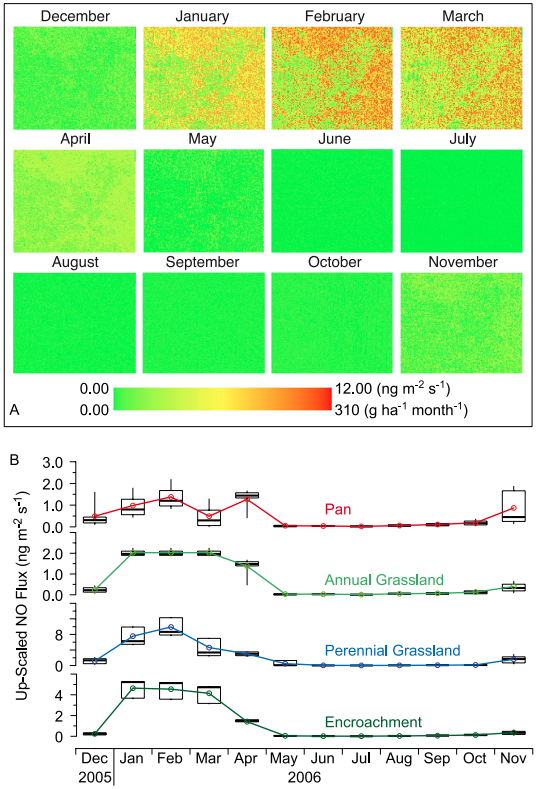

Fig. 11. (A) Estimation of the mean monthly up-scaled NO flux for the region of the southern Kalahari under investigation. These figs. occupy exactly the same area and are at the same resolution as Fig. 9 **(B)** monthly up-scaled NO fluxes from each of the vegetation patch types, the circle indicates the mean monthly up-scaled NO flux the solid bar indicates the median, the box indicates the region between the 25 and 75 percentiles nd the whiskers indicate the 10–90 percentile range.

BGD
5, 4621–4680, 2008

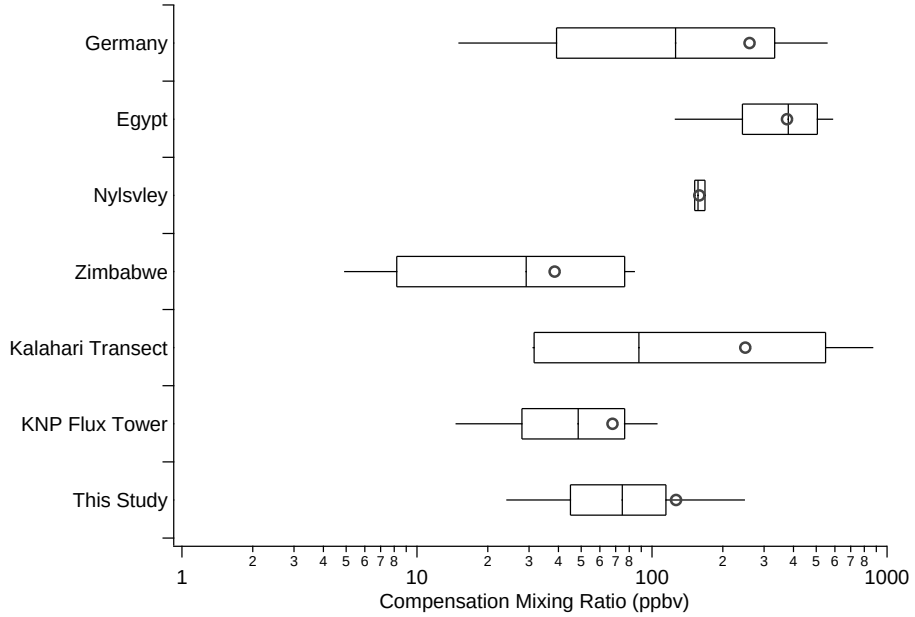

Fig. 12. Comparison of Compensation Mixing Ratio values reported in the literature. Circles represent the mean $m_{NO,comp}$ of the studies, the bar in the middle of the box represents the median mNO,comp, the box indicates the 25 and 75 percentiles and the whiskers represent the 10 and 90 percentile. Values for "Germany" are from (Bollmann et al., 1999; Gödde and Conrad, 1998; Gödde and Conrad, 1999; Rudolph and Conrad, 1996; Saad and Conrad, 1993), the values for "Egypt" are from (Saad and Conrad, 1993), Values for "Nylsvley" are from (Otter et al., 1999), values for "Zimbabwe" are from (Kirkman et al., 2001) and values for "KNP Flux Tower" are from (Feig et al., 2008).